Copy
RM L53G31a

NACA

RESEARCH MEMORANDUM

SUBSONIC AND SUPERSONIC HINGE-MOMENT AND EFFECTIVENESS

CHARACTERISTICS OF AN UNBALANCED LATERAL

CONTROL HAVING LOW THEORETICAL HINGE

MOMENTS AT SUPERSONIC SPEEDS

By Kennith L. Goin and William E. Palmer

Langley Aeronautical Laboratory
Langley Field, Va.

NATIONAL ADVISORY COMMITTEE
FOR AERONAUTICS

WASHINGTON
October 19, 1953

NATIONAL ADVISORY COMMITTEE FOR AERONAUTICS

RESEARCH MEMORANDUM

SUBSONIC AND SUPERSONIC HINGE-MOMENT AND EFFECTIVENESS

CHARACTERISTICS OF AN UNBALANCED LATERAL

CONTROL HAVING LOW THEORETICAL HINGE

MOMENTS AT SUPERSONIC SPEEDS

By Kennith L. Goin and William E. Palmer

SUMMARY

An experimental investigation has been made to determine the hinge-moment and effectiveness characteristics of a lateral control which has been shown by theoretical analysis to have low hinge moments due to deflection at supersonic speeds. The control, located at the tip of a clipped 60° delta wing, was of inversely tapered 60° half-delta plan form and was hinged about its leading edge. Its characteristics were determined through a subsonic Mach number range from 0.15 to 0.92 and at supersonic Mach numbers of 1.41, 1.62, and 1.96. At subsonic Mach numbers the test Reynolds numbers were 3.8×10^6 to 9.0×10^6 and at supersonic Mach numbers the test Reynolds numbers were 2.2×10^6 to 3.3×10^6.

As expected, the supersonic hinge-moment and rolling-moment characteristics of the control are predicted very well by linearized supersonic theory in the low deflection, low angle-of-attack range, thus lending support to the theoretical analysis from which the control was selected. Disagreements between experiment and theory at higher angles of attack and deflection are, however, sufficient to indicate limitations to the practical application of the analysis. Even at the higher angles of attack and deflection, the values of the supersonic hinge moments and deflection work of the control are much lower than those for a more conventional constant-chord unbalanced control. Values of supersonic deflection work for the subject tip control are also lower than those for a 100-percent overhang balance constant-chord control.

The differences between subsonic and supersonic hinge moments are considerably less for the tip control than those for more conventional unbalanced flap-type controls.

The control is in general effective in producing rolling moment throughout the range of the tests with the exception of angles of attack between 28° and 38° at low subsonic Mach numbers. For these conditions, with equal up and down deflection of opposite ailerons, the control effectiveness is reversed for low deflections but is again positive for large deflections.

The control could be used for moderate longitudinal trim changes; however, its effectiveness as a longitudinal trim device decreased with increasing Mach number.

INTRODUCTION

As an approach to the problem of reducing control hinge moments, a theoretical analysis was recently made to determine the plan forms of unbalanced trailing-edge flap-type controls which would have minimum hinge moments due to deflection at supersonic speeds (ref. 1). One interesting result of the analysis was the indication that on wings with unswept or sweptforward trailing edges, inversely tapered controls having triangular plan forms and highly sweptforward hinge lines would have maximum ratios of rolling moment to hinge moment.

In order to establish in some measure the reliability of the analysis, as well as to provide experimental information on this unusual type control, related investigations have been made in the Langley 9- by 12-inch supersonic blowdown tunnel at Mach numbers of 1.41, 1.62, and 1.96 and in the Langley low-turbulence pressure tunnel at Mach numbers from 0.15 to 0.92. The configuration tested at supersonic speeds consisted of a clipped 60° delta wing equipped with a half-delta control which had a 60° sweptforward hinge line and was located at the wing tip. The wing had NACA 65A003 airfoil sections parallel to the plane of symmetry. The subsonic configuration differed from the supersonic configuration mainly in that it had NACA 65A006 airfoil sections.

Tests at subsonic speeds were made at control deflections of -26° to 20°, angles of attack of -10° to 42° and Reynolds numbers of 3.8×10^6 to 9×10^6. Tests at supersonic speeds were made at control deflections of 0° to 20°, angles of attack of -12° to 12° and Reynolds numbers of 2.2×10^6 to 3.3×10^6.

SYMBOLS

The measured aerodynamic forces and moments were reduced to standard nondimensional coefficients so that all coefficients presented herein apply to the complete wing. The positive directions of forces, moments, and angles are shown in figure 1. The symbols and coefficients used herein are defined as follows:

b   model span for full-span model, twice model span for semispan model

c   local chord measured parallel to plane of symmetry

$\bar{c}$ mean aerodynamic chord, $\displaystyle\int_0^{b/2} c^2 dy \bigg/ \int_0^{b/2} c\, dy$

M   Mach number

M_a moment of area of aileron about hinge axis

p   roll velocity, radians/sec

q   free-stream dynamic pressure

R   Reynolds number, based on $\bar{c}$

S   model wing area

S_f control area

V   free-stream velocity

W   deflection work, $\displaystyle 2M_a q\left[\int_0^\delta C_h\, d\left(\frac{\delta}{57.3}\right) + \int_0^{-\delta} C_h\, d\left(\frac{\delta}{57.3}\right)\right]$

C_D drag coefficient, $\dfrac{\text{Drag}}{qS}$

C_h hinge-moment coefficient, $\dfrac{\text{Hinge moment}}{2M_a q}$

C_L lift coefficient, $\dfrac{\text{Lift}}{qS}$

C_l rolling-moment coefficient, $\dfrac{\text{Rolling moment}}{qSb}$

$C_{l_{gross}}$ gross rolling-moment coefficient,

$$\frac{\text{Rolling moment of semispan model}}{2qSb}$$

ΔC_l rolling-moment coefficient due to aileron deflection

$$C_{l_p} = \frac{\partial C_l}{\partial \left(\frac{pb}{2V}\right)}$$

C_m pitching-moment coefficient, $\dfrac{\text{Pitching moment about } \bar{c}/4}{qS\bar{c}}$

C_n yawing-moment coefficient, $\dfrac{\text{Yawing moment}}{qSb}$

C_Y lateral-force coefficient, $\dfrac{\text{Lateral force}}{qS}$

α angle of attack, deg

δ control deflection, measured in plane normal to hinge axis, deg

Subscripts:

α partial derivative of coefficient with respect to α

δ partial derivative of coefficient with respect to δ

APPARATUS AND TESTS

The full-span model used in the subsonic investigation and the semispan model used in the supersonic investigation both consist of bodies of revolution equipped with 60° delta wings having the tips cut off in the streamwise direction and having inversely tapered 60° half-delta controls located at the wing tips (figs. 2 to 4). The models have similar wing and control plan forms with the exception that the subsonic model has a tip fairing formed by revolution of the airfoil ordinates about the tip section, whereas the tip of the supersonic model is cut off squarely. The effect of the fairing is to give the subsonic model a taper ratio of 0.249, and an aspect ratio of 1.39 compared with a taper ratio of 0.262 and an aspect ratio of 1.35 for the supersonic

model. The subsonic wing has NACA 65A006 airfoil sections and the supersonic wing has NACA 65A003 airfoil sections parallel to the plane of symmetry. The ordinates of the bodies of revolution of the subsonic and supersonic models, are given respectively in reference 2 and in figure 4. The supersonic body had a cylindrical afterbody, whereas the subsonic body was boattailed.

Subsonic

Aileron installation.- The subsonic model is equipped with an aileron on the right wing. The aileron is attached to the wing by means of hinges which provide for control deflection and are instrumented with electrical strain gages for indicating hinge moments. The aileron has a radius nose. A gap of $0.001\bar{c}$ was maintained between the radius nose and adjacent wing during tests.

Tunnel.- The subsonic tests were conducted in the Langley low-turbulence pressure tunnel described in reference 3. Independent variations in Reynolds number and Mach number can be obtained by means of variation in tunnel stagnation pressure from 1 to 10 atmospheres in air and from 1/5 to 1 atmosphere in Freon-12. Mach numbers up to tunnel choke can be obtained with the use of Freon-12 as a testing medium. All data obtained in Freon-12 were converted to equivalent air data by the method of reference 4.

The model was sting mounted in the center of the tunnel as shown in figure 2(a). A six-component electrical strain-gage balance was housed within the model fuselage.

Corrections.- The effects on Mach number and dynamic pressure of constriction of the flow by the tunnel walls were taken into account by a method based on information presented in references 5 and 6. Angles of attack and drag coefficients were corrected for the effects of boundary induced upwash by the method of reference 7. Angles of attack have also been corrected for support deflection resulting from aerodynamic loading.

Supersonic

Aileron installation.- The supersonic model (shown in fig. 2(b)) was too thin in the vicinity of the hinge axis for installation of available electrical strain gages and resort was made to an optical system for measuring control hinge moments. In order to use this optical system, the wing and control were made from a single piece of steel which was weakened along the control hinge axis by grooves and

sawcuts as shown in figure 4. In this weakened condition the control deflected approximately 1/2° with respect to the wing at maximum hinge moment. The various control deflections were set by bending the model along the weakened hinge axis.

The model was aerodynamically faired in the vicinity of the hinge axis by use of balsa strips glued along the grooves. After tests had been made at $\delta = 0°$, the control was deflected 4° and hinge moments were measured with the sharp- and round-type fairings shown in figure 4. Data for the two types of fairing are compared in figure 5. Hinge moments for the sharp fairing indicate values of C_{h_δ} at $\alpha = 0°$ which are in good agreement with values calculated for a flat plate with a sharp bend at the hinge axis, whereas values of C_{h_δ} indicated for the round-type fairing are considerably more negative. Since the sharp-type fairing more nearly approximates the shape that would be expected to exist in practice, and since the analysis of reference 1 (from which this control was selected) is based on calculations for a flat plate with a sharp bend along the hinge axis, all subsequent tests were made with the sharp-type fairing.

It might be mentioned that, although differences in the aileron installations for the subsonic and supersonic tests may have some influence on the control characteristics, particularly hinge moments, such possible differences are not believed to be large enough to affect the general trends of the aileron characteristics with Mach number indicated by a comparison of the subsonic and supersonic data.

Tunnel.- The supersonic tests were conducted in the Langley 9- by 12-inch supersonic blowdown tunnel which utilizes the compressed air of the Langley 19-foot pressure tunnel. The compressed air is conditioned to insure condensation-free flow in the test section by being passed through a silica-gel drier and through banks of finned electrical heaters. Turbulence damping screens are located in the tunnel settling chamber. The absolute stagnation pressure of the air entering the test section is about 2 atmospheres. The three test-section Mach numbers are provided by use of interchangeable nozzle blocks. Deviations of the flow conditions in the test section, as determined from extensive calibration tests and reported in reference 8, are presented in the following table:

Average Mach number	1.41	1.62	1.96
Maximum deviation in Mach number	±.02	±.01	±.02
Maximum deviation in stream angle, deg	±.25	±.20	±.20

Test technique.- The semispan model was cantilevered from a five-component strain-gage balance which was set flush with the tunnel floor and was free to rotate through the angle-of-attack range. A half body of revolution was attached to the wing. A 0.25-inch shim was attached to the half body to raise it off the tunnel floor and thus minimize the effects of the tunnel-floor boundary layer on the flow over its surface. A description of the development of this shim is given in reference 9. A gap of about 0.01 inch was maintained between the test body and the tunnel floor.

Hinge moments were measured by using a modified version of the optical system described in reference 10. The system consisted of a single light source, three pairs of small mirrors imbedded in the top surface of the model along the hinge line, as shown in figure 4, and a translucent circular-arc screen on which light from the mirrors was reflected. The mirrors were set in the model with their faces parallel so that the relative positions of the three pairs of images on the screen directly indicated the deflection of the control relative to the wing, and consequently the control hinge moments. In order to keep the faces of the mirrors parallel, the mirrors in the control had to be reset each time the control deflection was changed, causing the top surface of the control to be uneven. However, in no case did the imbedded mirrors protrude above the surface of the model.

Accuracy

The magnitude of errors in the angular measurements and errors in aerodynamic coefficients resulting from general considerations of balance calibration accuracy, repeatability of data and accuracy of measurements is believed to be about as follows:

Variable	Error at subsonic Mach numbers	Error at supersonic Mach numbers
α, deg	± 0.1	± 0.05
δ, deg	0.2	0.25
C_L	0.010	0.005
C_D	0.001	0.001
C_m	0.003	-----
C_l	0.001	0.001
C_n	0.002	-----
C_Y	0.004	-----
C_h	0.008	0.010

The above value for δ for the supersonic tests is the error in initial control setting. Because of loading, there is an additional maximum variation of $\pm\frac{1}{2}^{o}$ in control deflection which has not been accounted for in the basic data plots of coefficient against angle of attack. In the cross plots of coefficient against δ, however, values of δ have been corrected for deflection under load.

The errors in C_D at subsonic and supersonic Mach numbers indicated in the preceding table apply only at low angles of attack. The error in C_D increases with increasing α because of the greater contribution of the normal force to the drag. The balances used for both the subsonic and supersonic tests measured normal and chord forces which were converted to lift and drag for this report. The relative accuracy of the supersonic pitching-moment measurements (the accuracy of each data point with respect to each other data point at the same lift coefficient) is believed to be about 0.002 in terms of C_m. The absolute accuracy of the measurements is not known, however, because, subsequent to the measurements, the balance was modified and since the modification the pitching-moment data of this report cannot be repeated. There is a consistent unexplained discrepancy between data obtained before and after the modification which amounts to an indicated difference in aerodynamic-center location of approximately 0.05 inch ($0.01\bar{c}$).

RESULTS AND DISCUSSION

Lateral and Hinge-Moment Characteristics

The basic lateral force and moment and hinge-moment coefficients plotted against angle of attack are presented in figures 6 to 9.

Lateral force.- The subsonic lateral-force data of figure 6 show maximum increments of C_Y resulting from control deflection of about 0.01 at positive angles of attack up to the stall, which occurs between about 28° and 32°. Maximum increments in C_Y at these angles are produced by positive control deflections. The large deviations at high angles of attack of lateral-force curves from zero at zero deflection shown in figure 6 are characteristic of wings of delta and modified delta plan forms. It is believed that, since there was a gap between the control and the wing on only one wing, there were consistent flow differences between the two wings which influenced the direction of this deviation. Similar deviations of C_l and C_n are also indicated in figures 6 and 8.

Yawing moments.- The subsonic yawing-moment data of figure 8 show that yawing-moment increments due to control deflection are in general slightly negative for positive control deflections and near zero for negative deflections at angles of attack up to 20° or above. Although the increments due to positive deflection are negative, indicating slightly favorable yawing moments, the magnitudes of the increments are approaching the accuracy of the data.

Rolling moment.- One interesting result illustrated by the subsonic rolling-moment data of figure 6 is that control effectiveness increases at both negative and positive deflections as angle of attack is increased from 0° and reaches a maximum at angles of attack between about 10° and 20°.

At Mach numbers of 0.15 and 0.40, the data of figure 6 show that the control is effective at all deflections at angles of attack up to about 28°. As the angle of attack approaches that for stall ($\alpha = 28^\circ$ to 32°) the effectiveness decreases and reversals occur at low negative deflections and at all positive deflections at angles of attack between 28° and 38°. High negative deflections are effective at all angles of attack and all deflections again become effective as the angle of attack is increased to 40° or above.

At Mach numbers between 0.60 and 0.92, the data of figure 6 show that in general the control is effective at all deflections at all angles of attack up to the maximum of the tests. The effectiveness at angles of attack greater than 20° is less than the maximum effectiveness at somewhat lower angles of attack but is generally greater than at $\alpha = 0^\circ$.

The subsonic rolling-moment data of figure 6, together with the supersonic rolling-moment data of figure 7 are summarized in figure 10 in the form of crossplots of ΔC_l against δ. The crossplots of figure 10 for the supersonic Mach numbers present data for negative control deflections which were obtained by reversing the signs of α, δ, and C_l. This method of handling the data was possible because the model is symmetrical about its chord plane. Figure 10 illustrates the previously mentioned increases in effectiveness with increases in angle of attack at subsonic Mach numbers and show similar though smaller increase at supersonic Mach numbers.

The comparison in figure 10 of experimental and theoretical values of rolling-moment coefficient at supersonic speeds shows very good agreement at $\alpha = 0^\circ$. At higher angles of attack, however, the experimental rolling moments are somewhat higher than predicted. The good agreement of theory with experiment at $\alpha = 0^\circ$ lends support to the analysis of

reference 1, from which this control was selected, whereas the disagreement at the higher angles of attack indicates limitations to the practical application of the analysis.

Hinge moment.- The hinge-moment data of figures 8 and 9 indicate hinge-moment variations with angle of attack which are very similar at subsonic and supersonic speeds. Through a limited range of angle of attack near 0°, values of C_{h_α} are relatively low. As the angle of attack is increased beyond this range there is a negative increase in C_{h_α} followed by a general decrease. Although the trends are similar, the slopes of the C_h against α curves are much more negative at supersonic speeds than at subsonic speeds.

The crossplots of figure 11 indicate trends of hinge-moment variations with control deflection which are similar at subsonic and supersonic speeds. At $\alpha = 0^O$ and low control deflections, values of C_{h_δ} are relatively low. As the deflection is increased at $\alpha = 0^O$, values of C_{h_δ} increase. At subsonic speeds the slopes of the C_h against δ curves in general tend to increase continuously with increases in angle of attack up to 25°. At supersonic speeds, however, there is an increase as α is increased from 0° to 4° but further increases in α to 12° have little effect on C_{h_δ}.

The comparisons of theoretical and experimental hinge moments at supersonic speeds (fig. 11) show that theory predicts the hinge moments very well in the range where theory would be expected to be applicable, that is, at $\alpha = 0^O$ and at values of δ near zero. The theoretical values of C_{h_δ} are, however, considerably less negative than experimental values at higher deflections at $\alpha = 0^O$ and at all deflections at higher angles of attack.

Evaluation of control hinge-moment characteristics.- Figure 12 has been prepared in order to evaluate to some measure the characteristics of the control under practical conditions. The upper plot presents values of C_l which were estimated to be required to produce a roll rate of the subject wing of 3.5 radians per second (assuming a 30-foot wing span and an altitude of 40,000 feet). Also presented in the upper plot in figure 12 are similar values of C_l for a 60° delta wing (of area equal to that of the subject wing) having a constant-chord flap-type control which will be used for comparative purposes. The calculated values of C_l required were obtained by use of theoretical values

of C_{l_p} from references 11 and 12. It should be pointed out that cal-

culated values of C_l do not take into account the effects of wing twist on aileron effectiveness, the effects of angle of attack on C_{l_p}, and other factors which might be of importance in practice. However, the variation with Mach number of the required rolling moment would be expected to be fairly typical if a constant rate of roll is the criterion.

The other two plots of figure 12 present experimental values of C_h against Mach number for equal up and down deflections of opposite ailerons producing the estimated required rolling moment. The static data of this figure were obtained by use of static values of hinge-moment and rolling-moment coefficient and are representative of the case in which the controls are fully deflected before the aircraft starts to roll. This case is the one for which the hinge moments of unbalanced controls, which have negative values of C_{h_α}, will be maximum, because as soon as the aircraft starts to roll there will be a balancing effect on control hinge moments. In order to give some indication of these balancing effects due to rolling, values of C_h for the steady-roll case are also presented. Values of C_h for the steady-roll case were obtained by determining the equal up and down deflections which produce the required values of C_l by determining the induced angle of attack at the centroid of the control for a roll rate of 3.5 radians per second, by assuming the effective angle of attack to be the initial angle of attack plus this induced angle of attack, and by determining the net hinge-moment coefficients at the effective angles of attack. As pointed out previously, the calculations for the rolling case do not take into account several factors which might be of importance in practice. However, it is believed that the data obtained will give a reasonable indication of the magnitude of the effects of rolling on the hinge moments. The negative sign of C_h indicates underbalanced hinge moments.

Values of C_h are shown for the subject control at $\alpha = 0^o$ and 8° and are compared with similar values for the more familiar unbalanced constant-chord flap-type control. The ratio of control area to wing area for the constant-chord control is approximately equal to that of the sub-ject control. Data for the constant-chord control are unpublished data from tests of a semispan model in the Langley 9- by 12-inch supersonic blowdown tunnel. The subsonic data for this control do not include reflection plane or jet-boundary corrections.

Probably the most significant result indicated by figure 12 is that differences between subsonic and supersonic hinge moments for the subject control are considerably less than those for the more familiar constant-chord

control. The relatively small changes in hinge moments for the subject
control can probably be attributed mainly to the fact that the leading
edge of the control is subsonic throughout the Mach number range of the
investigation and consequently that the control does not experience the
radical changes in loading of the unswept constant-chord controls. This
feature would appear to indicate that the aerodynamic problems involved
in balancing this type control would be less complex than for flap-type
controls having low to moderate amounts of leading-edge sweep.

The data of figure 12 show that values of C_h for the subject con-
trol are considerably less than those for the unbalanced control which
was not designed to have low hinge moments. Because the value of M_a
(on which values of C_h are based) for the subject control is about $4/3$
that of the constant-chord control, the differences between the hinge
moments of the two is not quite as great as indicated by the values of
C_h. However, at supersonic speeds, the hinge moments of the subject con-
trol are much lower than those of the constant-chord control.

The data of figure 12 indicate that an appreciable amount of balance
due to steady roll is obtained for the subject control at $\alpha = 0^O$ and
that a considerably greater amount of balance is obtained at $\alpha = 8^O$. In
fact, at $\alpha = 8^O$, approximately zero hinge moments are shown at subsonic
speeds. The balancing effects of the constant-chord control due to steady
rolling are much less than those for the subject control.

Evaluation of deflection work characteristics.- In addition to hinge
moments, which are important as such when the strength of the actuating
mechanism or the amount of torque available at the control is the criterion
the work required to overcome the hinge moments due to deflection is an
important consideration since it determines the amount of energy which must
be supplied to the power-boost system. In order to examine the deflection
work characteristics of the subject control, plots of W corresponding to
the static C_h data of figure 12 have been prepared and are presented in
figure 13. In addition to data for the two unbalanced controls, values
of W at supersonic speeds are also presented for a 100-percent overhang
balanced control which was obtained by shifting the hinge axis of the
unbalanced constant-chord control to the half-chord location.

The data of figure 13 show that the unbalanced constant-chord control
requires deflection work about equal to that of the subject control at
subsonic speeds but considerably more work than the subject control at
supersonic speeds. Figure 13 also shows that at supersonic speeds, the
deflection work for the balanced control is considerably greater than for
the subject control except at $\alpha = 0^O$ at the lowest Mach number investi-
gated. These results indicate that from the standpoint of work required for
lateral control, the unbalanced and the 100-percent overhang balanced
constant-chord controls are decidedly inferior to the subject control at

supersonic speeds. Additional points showing the effects of rolling at $M = 1.96$ indicate that the comparison of deflection work for the three ailerons considered is not appreciably affected by the rolling condition.

It is of interest to note that the advantages of the 100-percent balanced control over the unbalanced constant-chord control, using low values of W as the criterion, are appreciable at $\alpha = 0^\circ$ but are relatively small at $\alpha = 8^\circ$.

Longitudinal Characteristics

Plots of C_L against α, C_m, and C_D are presented in figures 14 and 15 for representative subsonic and supersonic Mach numbers. The data indicate that the control would not be very effective as a flap since the maximum increase in lift coefficient due to 20° deflection is about 0.04. The data indicate, however, that the control could be used for moderate longitudinal trim changes. The effectiveness of the control as a longitudinal trim device is shown to decrease as Mach number increases.

The subsonic data indicate that at positive lift coefficients there is little if any increase in drag at a given lift coefficient due to positive control deflections. Negative deflections, however, resulted in drag increases. The supersonic data indicate that at both positive and negative lift coefficients, drag increases resulted from positive control deflections. The significance of the lift, drag, and pitching-moment characteristics with regard to the use of the tip control as a longitudinal control device, will depend mainly on the specific application and, therefore, no attempt has been made to evaluate fully these characteristics.

CONCLUDING REMARKS

Tests at subsonic and supersonic speeds of a clipped 60° delta wing equipped with an inversely tapered 60° half-delta control located at its tip have indicated the following results:

As expected, the supersonic hinge-moment and rolling-moment characteristics of the control are predicted very well by linearized supersonic theory in the low deflection, low angle-of-attack range, thus lending support to the theoretical analysis from which the control was selected. Disagreements between experiment and theory at higher angles of attack and deflection are, however, sufficient to indicate limitations to the practical application of the analysis. Even at the higher angles of attack and deflection, the values of supersonic hinge moments and deflection work of the control are much lower than those for a more conventional constant-chord unbalanced control. Values of supersonic deflection work

CONFIDENTIAL

for the subject control are also lower than those for a 100-percent overhang balance constant-chord control.

The differences between subsonic and supersonic hinge moments are considerably less for the tip control than those for more conventional unbalanced flap-type controls. This feature would appear to indicate that the aerodynamic problems involved in balancing this type control throughout the speed range would be less complex than in the case of more conventional flap-type controls.

The control is in general effective in producing rolling moment throughout the range of the investigation with the exception of angles of attack between 28° and 38° at low subsonic Mach numbers. For these conditions, with equal up and down deflection of opposite ailerons, the control effectiveness is reversed for low deflections but is again positive for large deflections.

The control could be used for moderate longitudinal trim changes; however, its effectiveness as a longitudinal trim device decreased with increasing Mach number.

Langley Aeronautical Laboratory,
        National Advisory Committee for Aeronautics,
                Langley Field, Va., August 10, 1953.

REFERENCES

1. Goin, Kennith L.: Theoretical Analysis To Determine Unbalanced Trailing-Edge Controls Having Minimum Hinge Moments Due to Deflection at Supersonic Speeds. NACA RM L51F19, 1952.

2. Osborne, Robert F., and Mugler, John P., Jr.: Aerodynamic Characteristics of a 45° Sweptback Wing-Fuselage Combination and The Fuselage Alone Obtained in the Langley 8-Foot Transonic Tunnel. NACA RM L52E14, 1952.

3. Von Doenhoff, Albert E., and Abbott, Frank T., Jr.: The Langley Two-Dimensional Low-Turbulence Pressure Tunnel. NACA TN 1283, 1947.

4. Von Doenhoff, Albert E., and Braslow, Albert L.: Studies of the Use of Freon-12 As a Testing Medium in the Langley Low-Turbulence Pressure Tunnel. NACA RM L51I11, 1951.

5. Herriot, John G.: Blockage Corrections for Three-Dimensional-Flow Closed-Throat Wind Tunnels, With Consideration of the Effect of Compressibility. NACA Rep. 995, 1950. (Supersedes NACA RM A7B28.)

6. Glauert, H.: Wind Tunnel Interference on Wings, Bodies and Airscrews. R. & M. No. 1566, British A.R.C., 1933.

7. Katzoff, S., and Hannah, Margery E.: Calculation of Tunnel-Induced Upwash Velocities for Swept and Yawed Wings. NACA TN 1748, 1948.

8. May, Ellery B., Jr.: Investigation of the Effects of Leading-Edge Chord-Extensions on the Aerodynamic and Control Characteristics of Two Sweptback Wings at Mach Numbers of 1.41, 1.62, and 1.96. NACA RM L50L06a, 1951.

9. Conner, D. William: Aerodynamic Characteristics of Two All-Movable Wings Tested in the Presence of a Fuselage at a Mach Number of 1.9. NACA RM L8H04, 1948.

10. Guy, Lawrence D.: Control Hinge-Moment and Effectiveness Characteristics of a 60° Half-Delta Tip Control on a 60° Delta Wing at Mach Numbers of 1.41 and 1.96. NACA RM L52H13, 1952.

11. Polhamus, Edward C.: A Simple Method of Estimating the Subsonic Lift and Damping in Roll of Sweptback Wings. NACA TN 1862, 1949.

12. Malvestuto, Frank S., Jr., Margolis, Kenneth, and Ribner, Herbert S.;
    Theoretical Lift and Damping in Roll at Supersonic Speeds of Thin
    Sweptback Tapered Wings With Streamwise Tips, Subsonic Leading
    Edges, and Supersonic Trailing Edges. NACA Rep. 970, 1950.
    (Supersedes NACA TN 1860.)
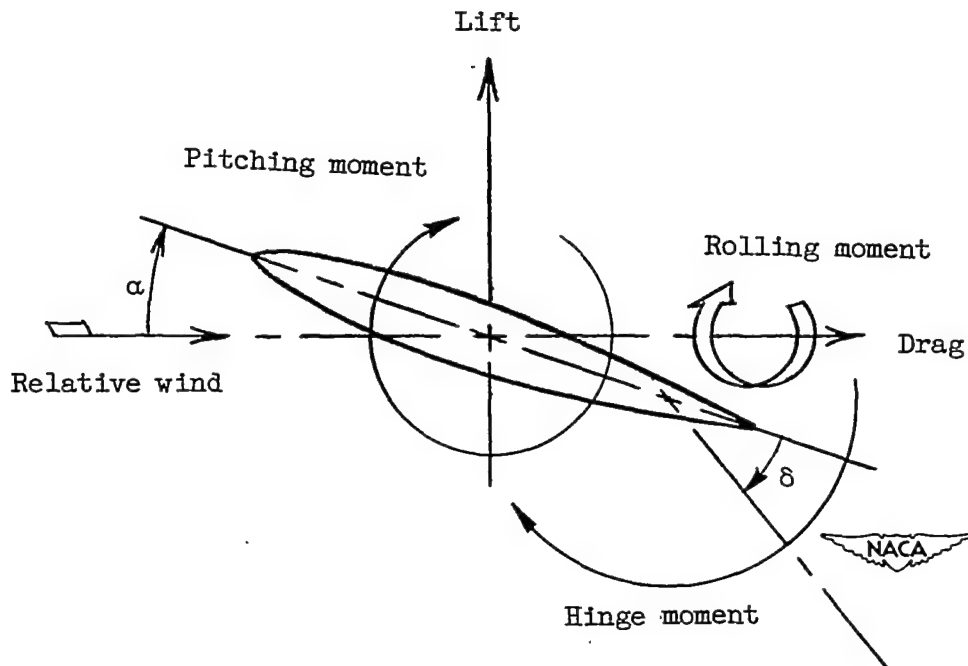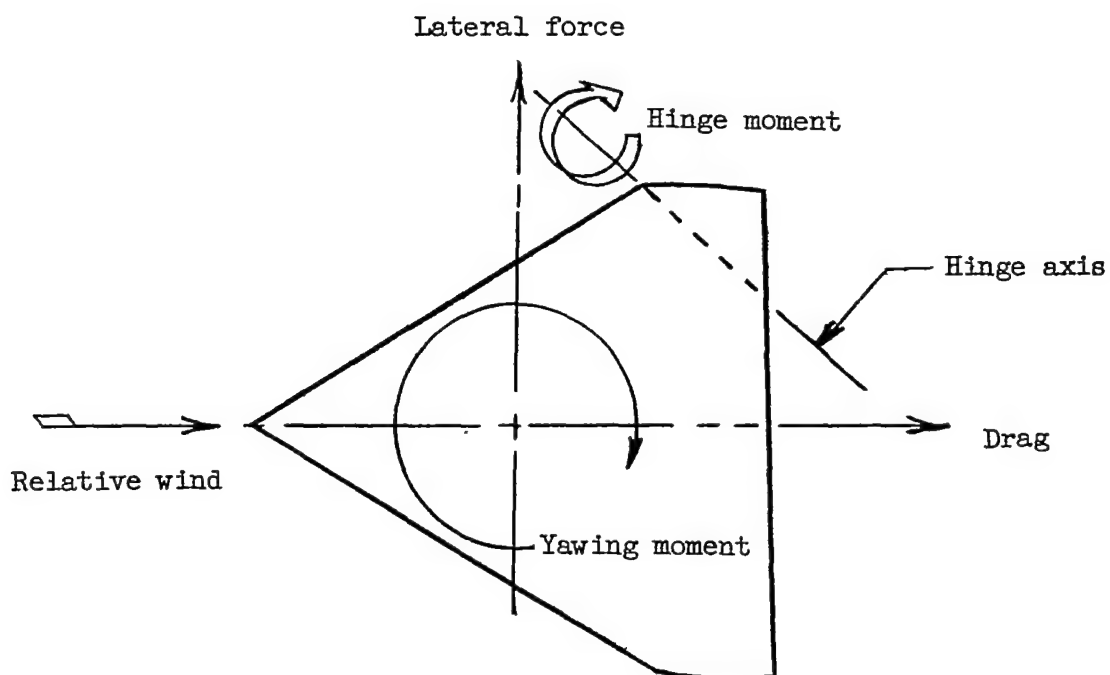
Figure 1.- System of axes used. Forces, moments, and angles are considered
positive in the directions indicated.

NACA RM L53G31a
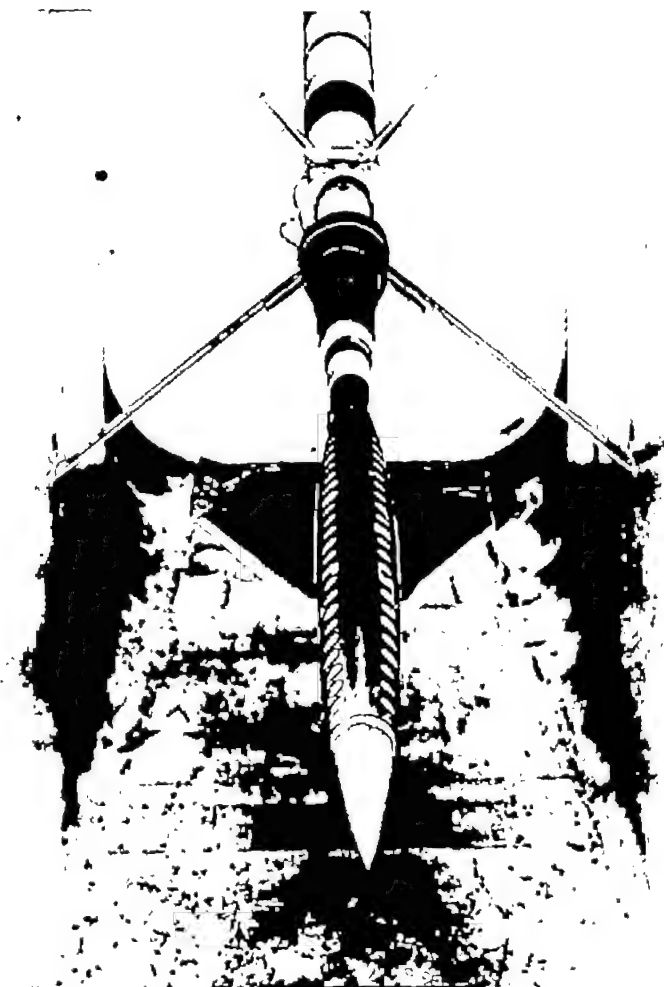
L-76918

(a) Subsonic model.

Figure 2.- Photographs of the models.

L-80534

(b) Supersonic model.

Figure 2.- Concluded.

Model Details

Airfoil section
  parallel to airstream   NACA 65A006
Area, sq. ft.   0.937
$\bar{c}$, in.   11.06
Sweepback (c/4), deg.   52.4
Aspect ratio   1.39
Taper ratio   0.249
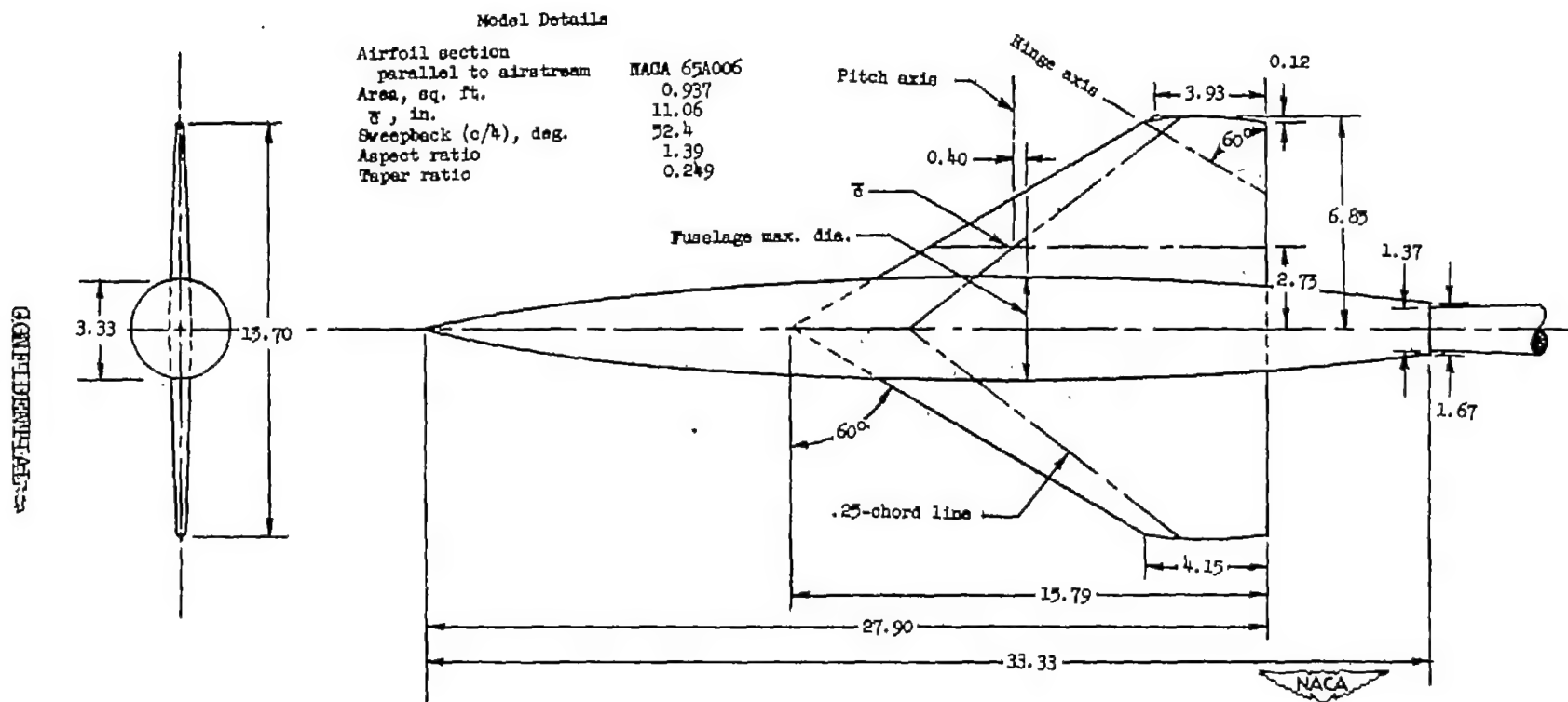
Figure 3.- Diagram of the model used in the subsonic tests. All
dimensions are in inches.

Saw cut
0.073 diam. mirror
Groove

A

A

Details of Tip

0.125 radius

.020

Sections A-A

Balsa fairing (round)

δ

Balsa fairing (sharp)

δ

Model Details

Airfoil section parallel to air stream   NACA 65A003
Half area, sq. in.   13.46
c̄   4.98
Sweepback (c/4), deg   52.4
Aspect ratio   1.35
Taper ratio   0.262

Hinge line

1.857

60°

3.013

Fuselage x	Ordinates r
0	0
.541	.094
1.082	.180
1.623	.260
2.165	.330
2.706	.391
3.247	.444
3.788	.490
4.330	.519
4.870	.538
5.412	.541
9.000	.541

Direction of flow

60°

x

0.25 shim

0.007 to 0.015
clearance gap

1.549

3.346

7.078

9.000

Rolling-moment axis

Tunnel floor

Pitching moment ref. axis

NACA

Figure 4.- Details of semispan model tested at supersonic speeds. All
dimensions are in inches.

Hinge-moment coefficient, C_h

M
1.41
1.62
1.96

Balsa fairing (round)

δ

Balsa fairing (sharp)

δ

Hinge line

Wing chord plane

Angle of attack, α, deg
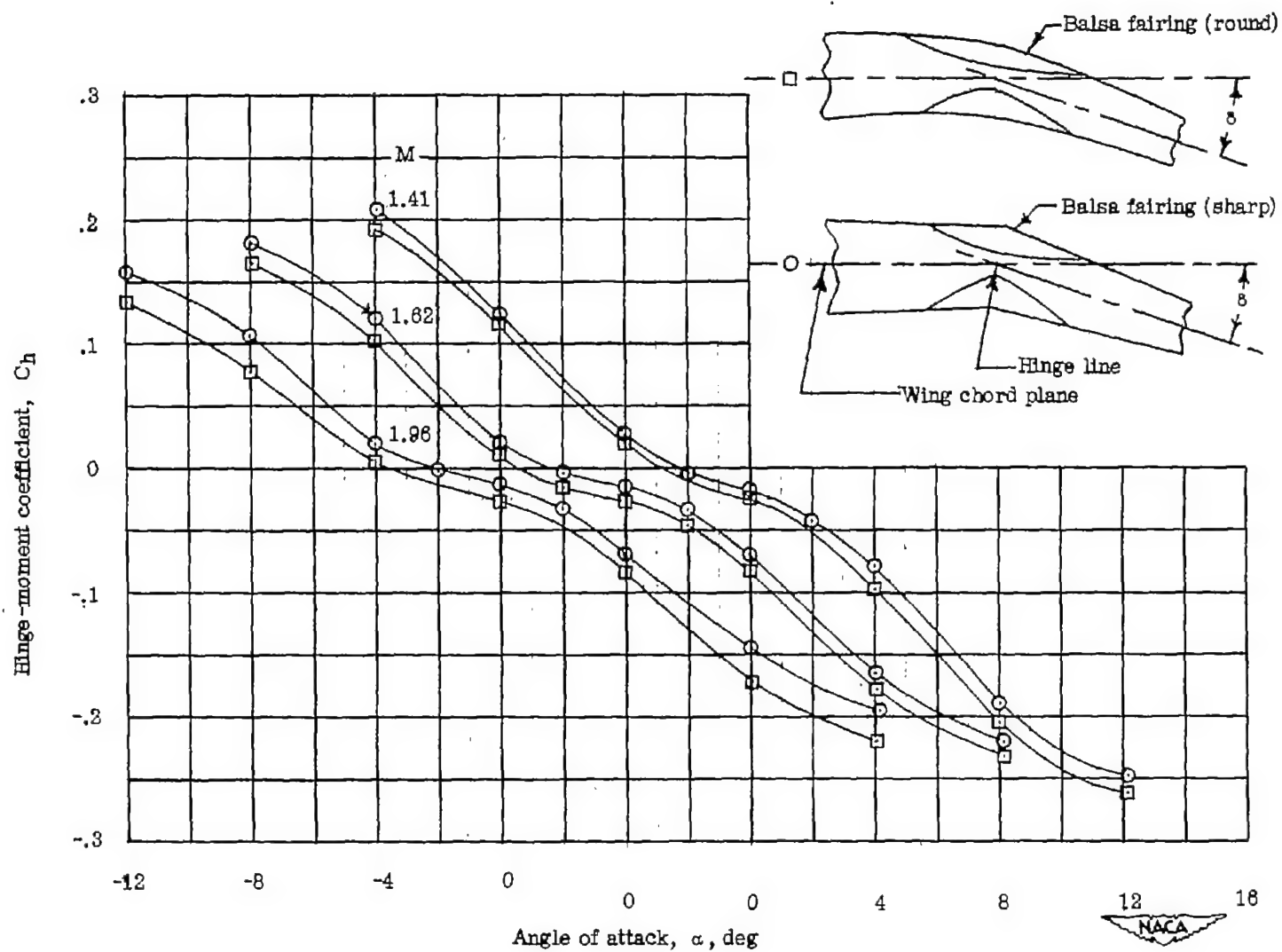
Figure 5.- Control hinge moments at $\delta = 4^\circ$ with two types of aerodynamic fairing in the vicinity of the hinge axis.
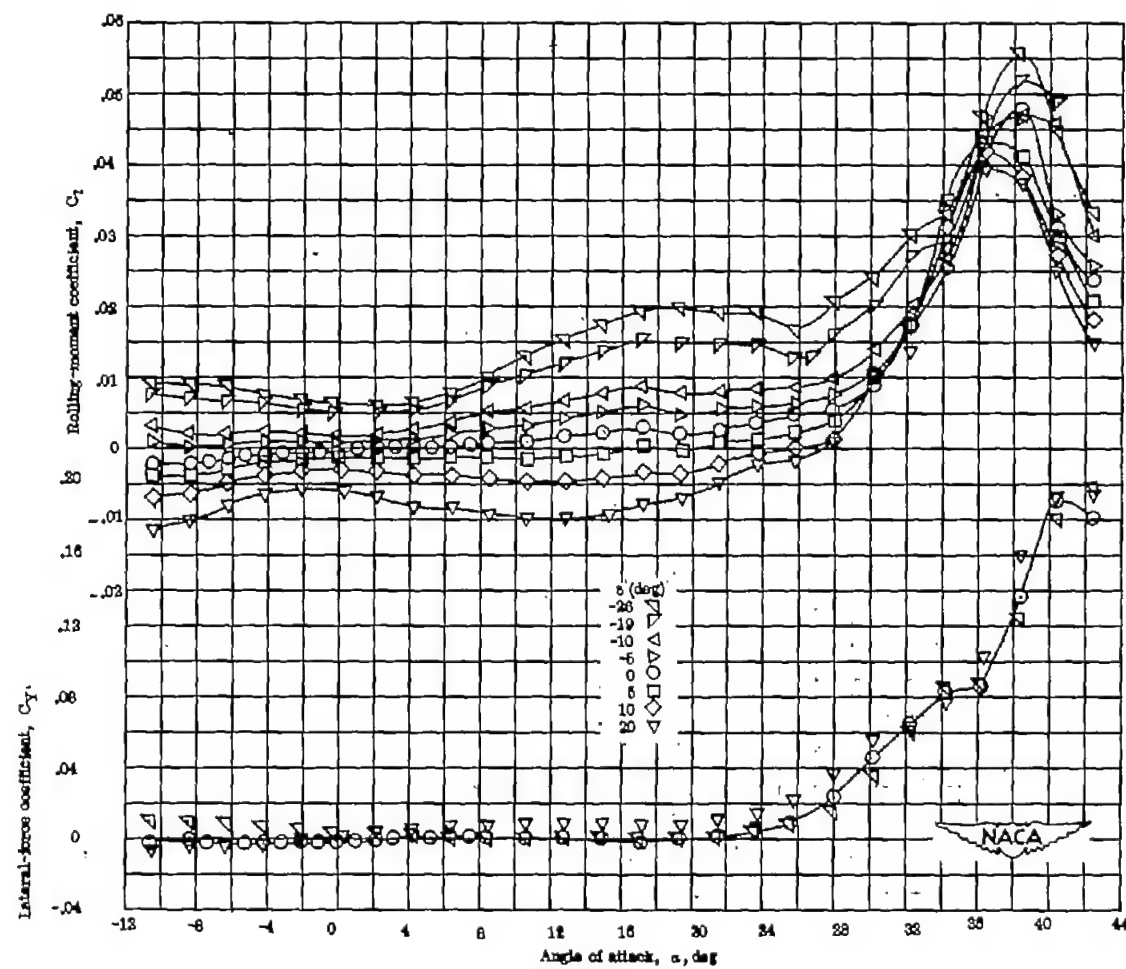
(a) M = 0.15; R = 9 × 10^6.

Figure 6.- Rolling-moment and lateral-force characteristics at subsonic
speeds.
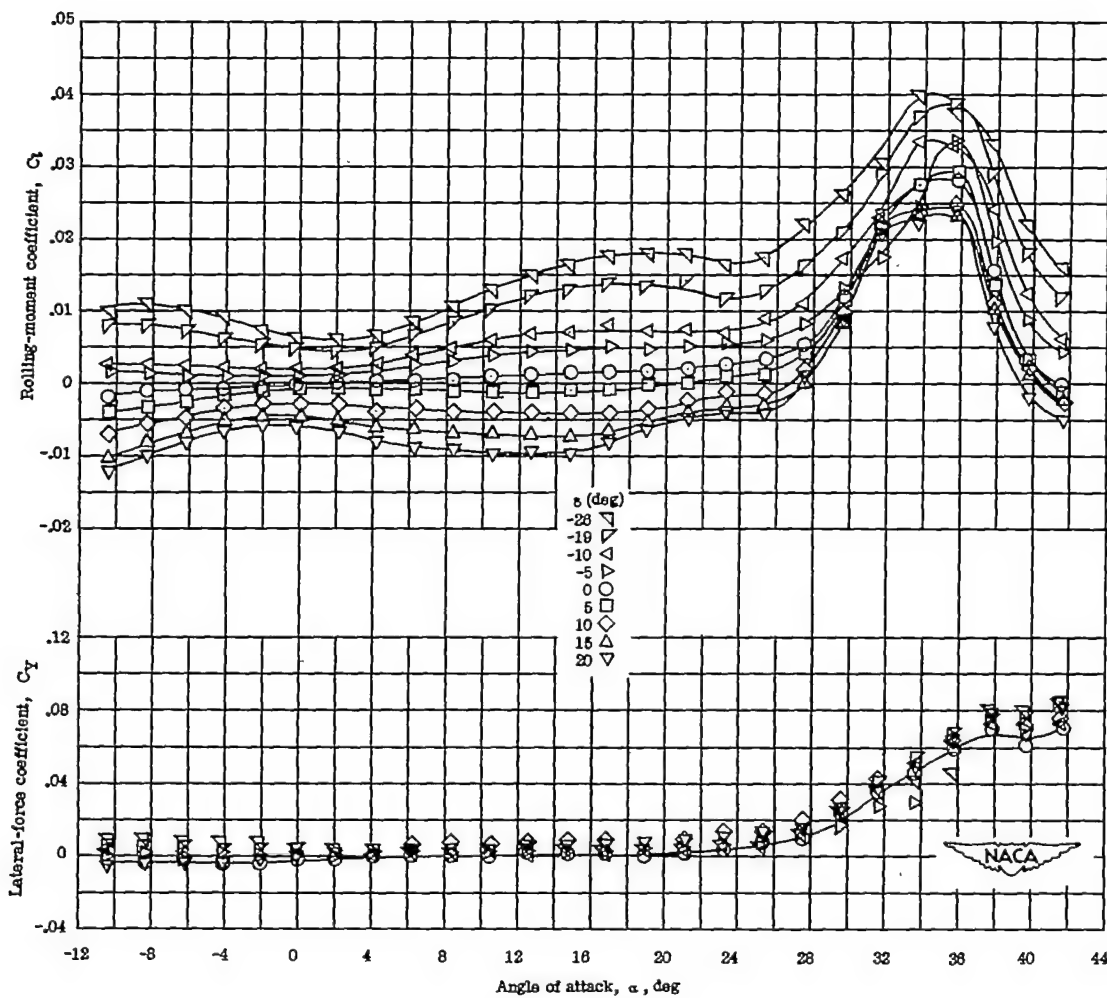
(b)   M = 0.4; R = 3.8 × 10⁶.

Figure 6.- Continued.
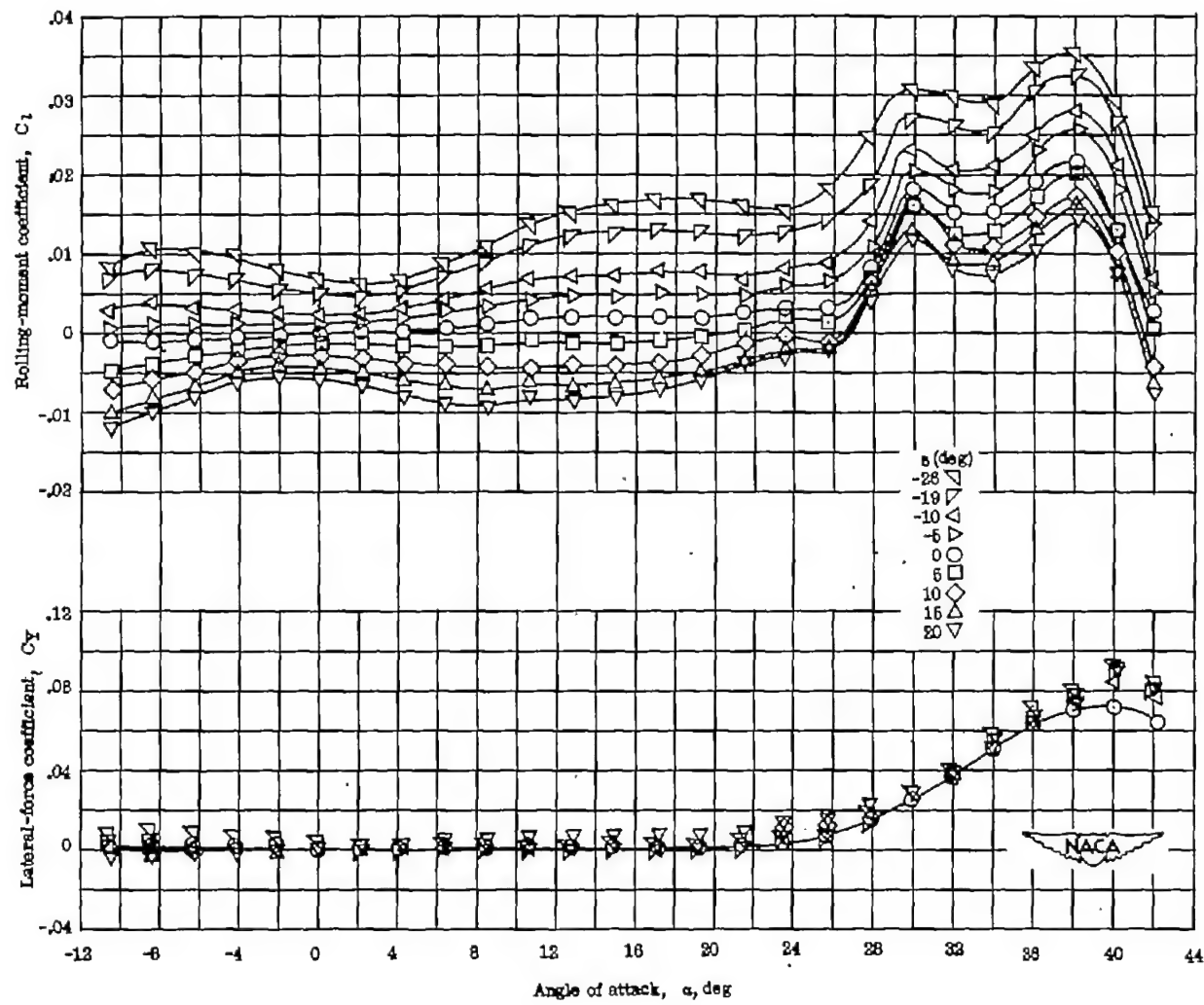
(c) M = 0.6; R = 5.1 × 10^6.

Figure 6.- Continued.
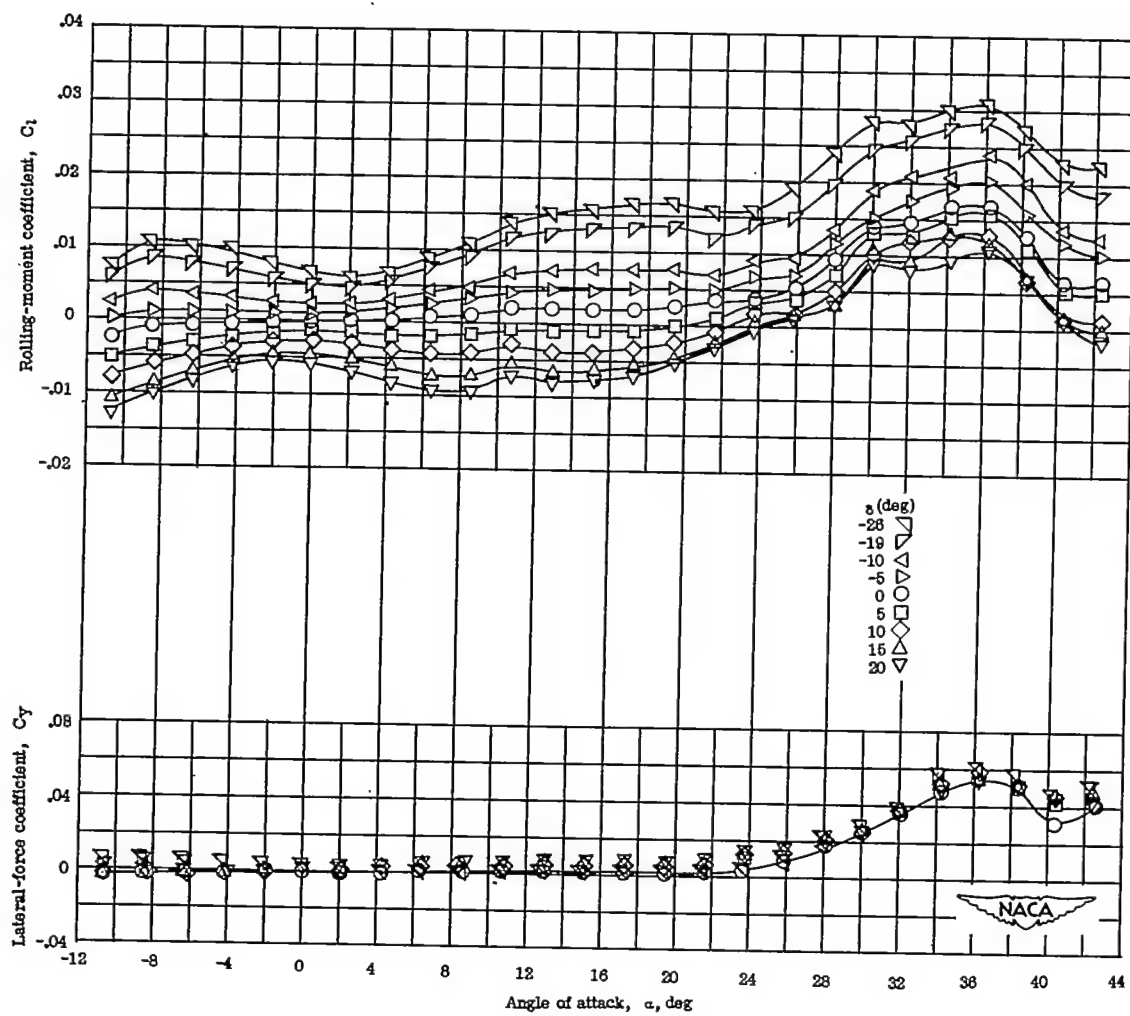
(d) M = 0.7; R = 5.5 × 10^6.

Figure 6.- Continued.
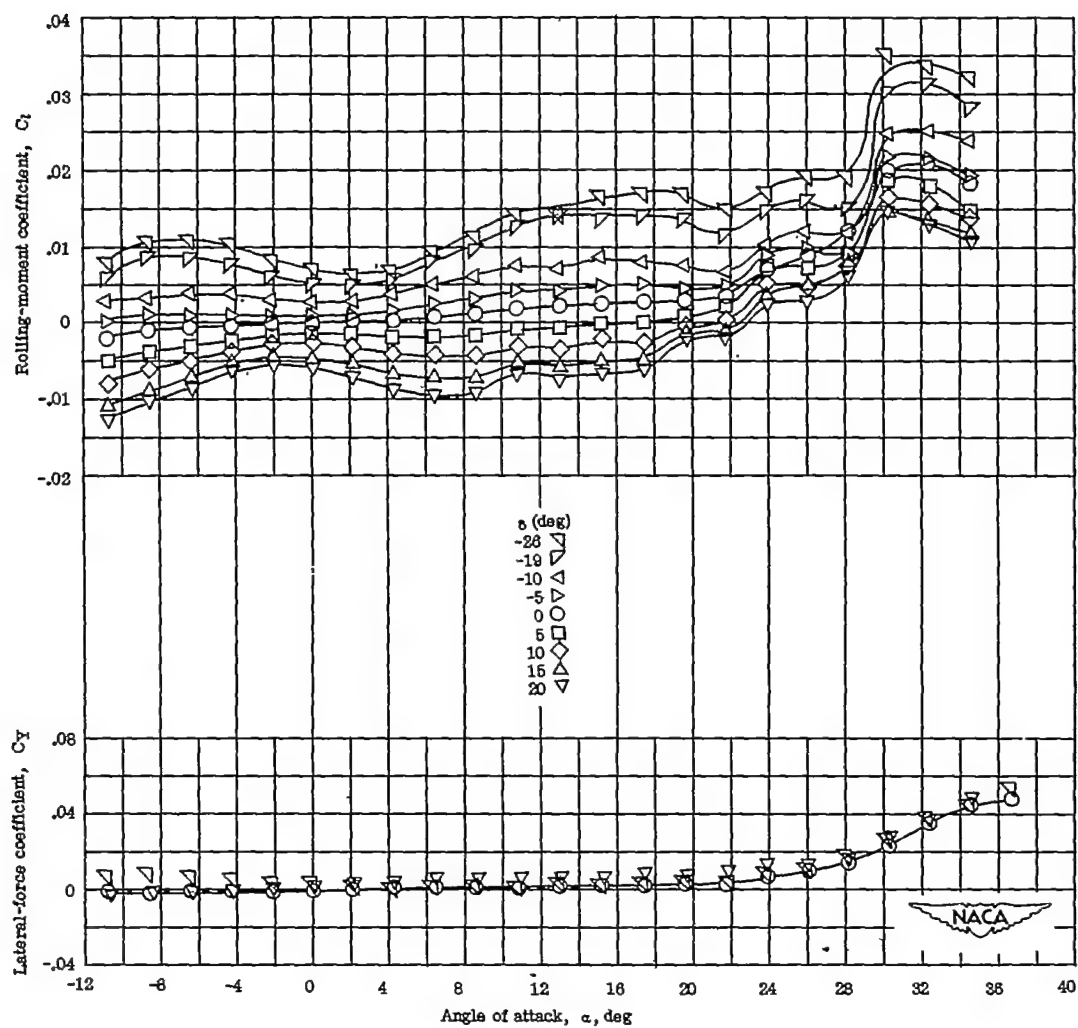
(e) $M = 0.8$; $R = 6 \times 10^6$.

Figure 6.- Continued.
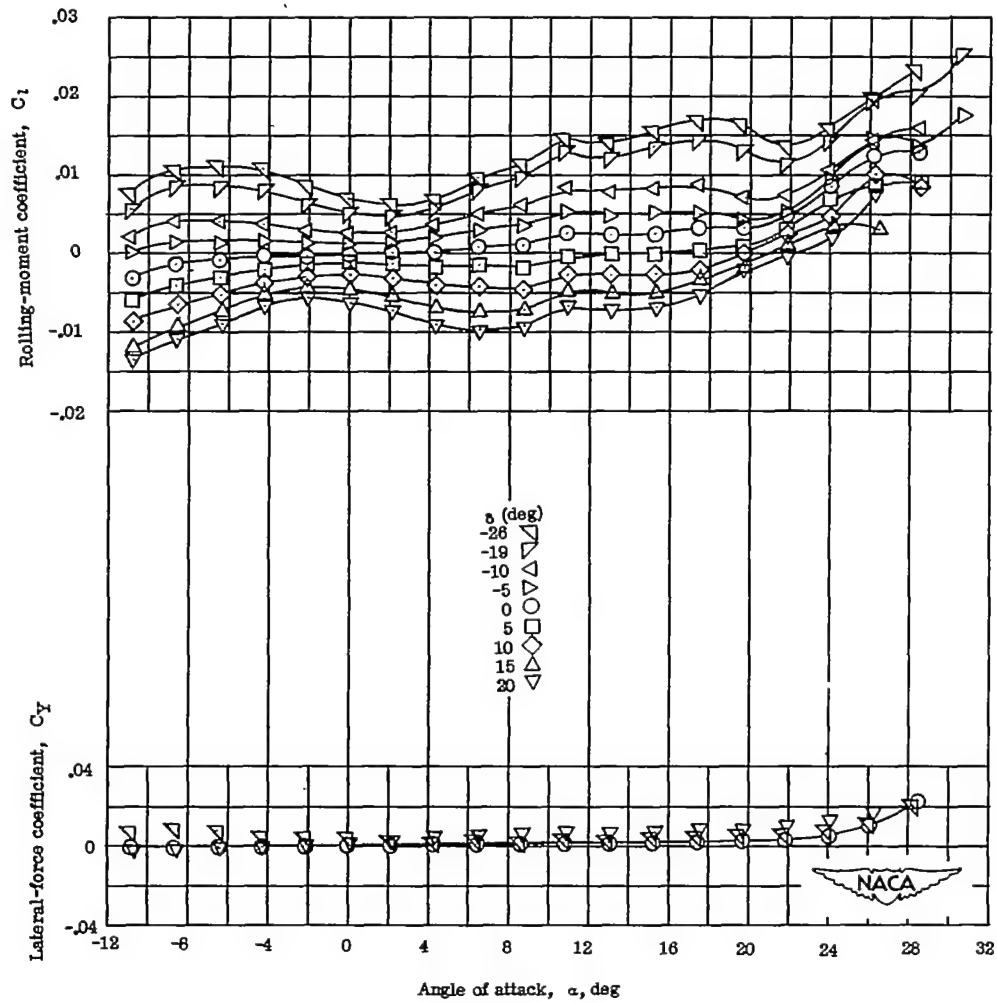
(f) M = 0.85; R = 6.1 × 10^6.

Figure 6.- Continued.
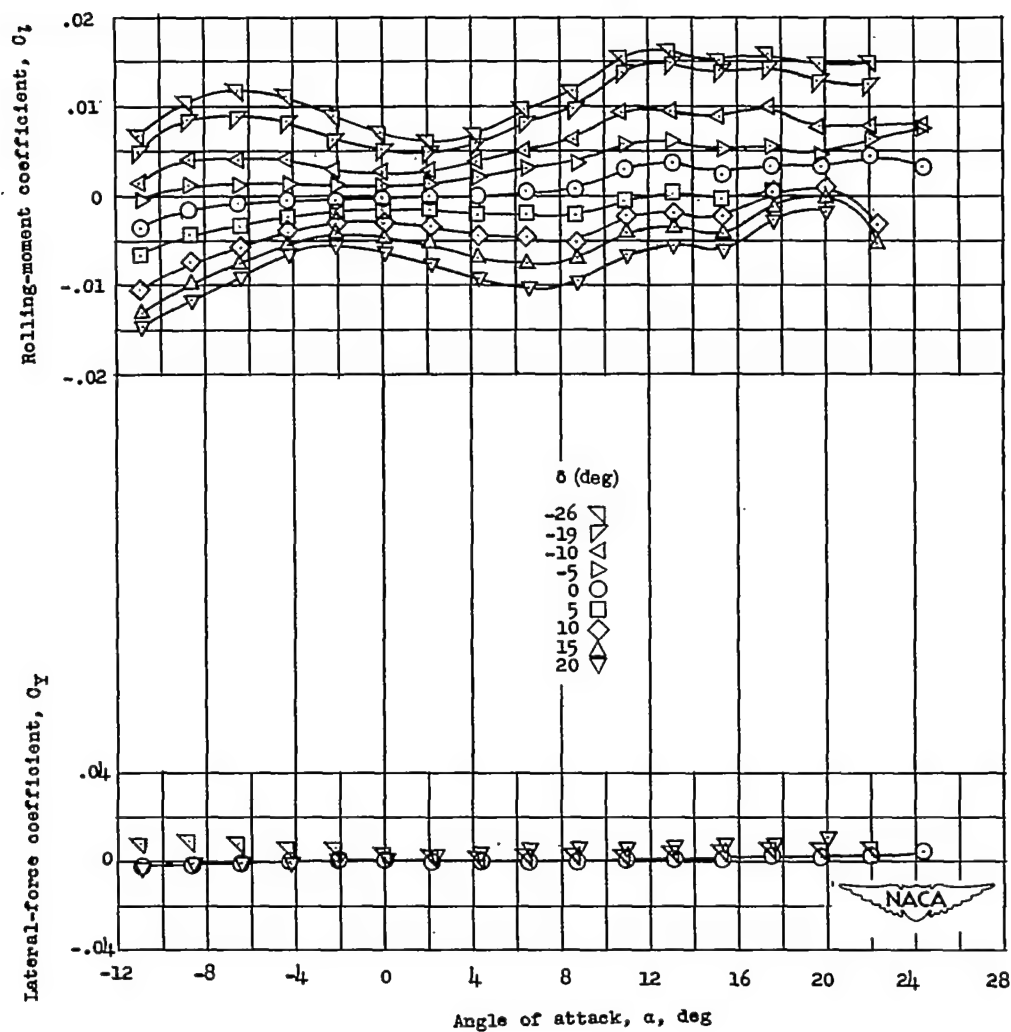
(g) M = 0.875; R = 6.2 × 10⁶.

Figure 6.- Continued.
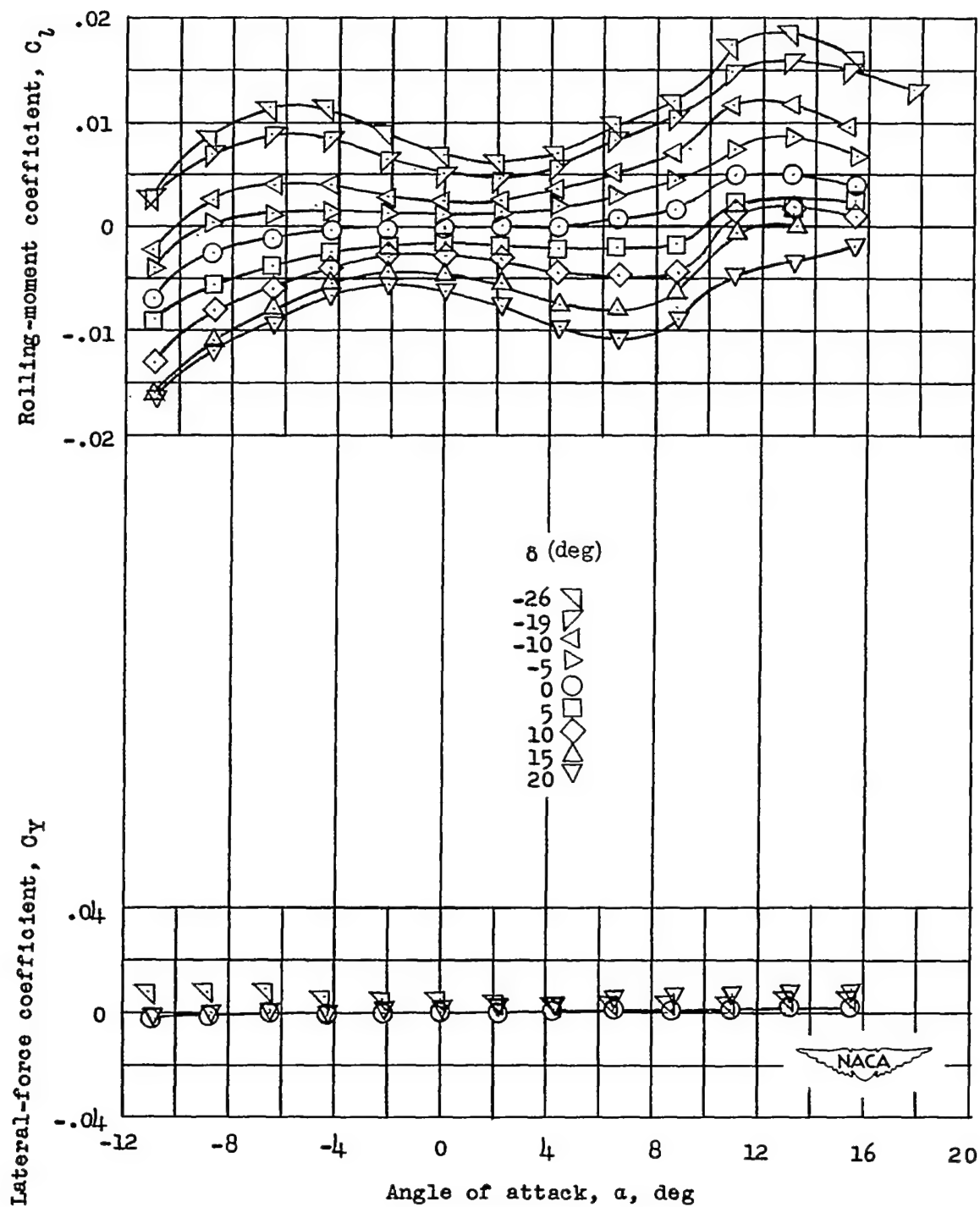
(h) M = 0.9; R = 9.3 × 10^6.

Figure 6.- Continued.
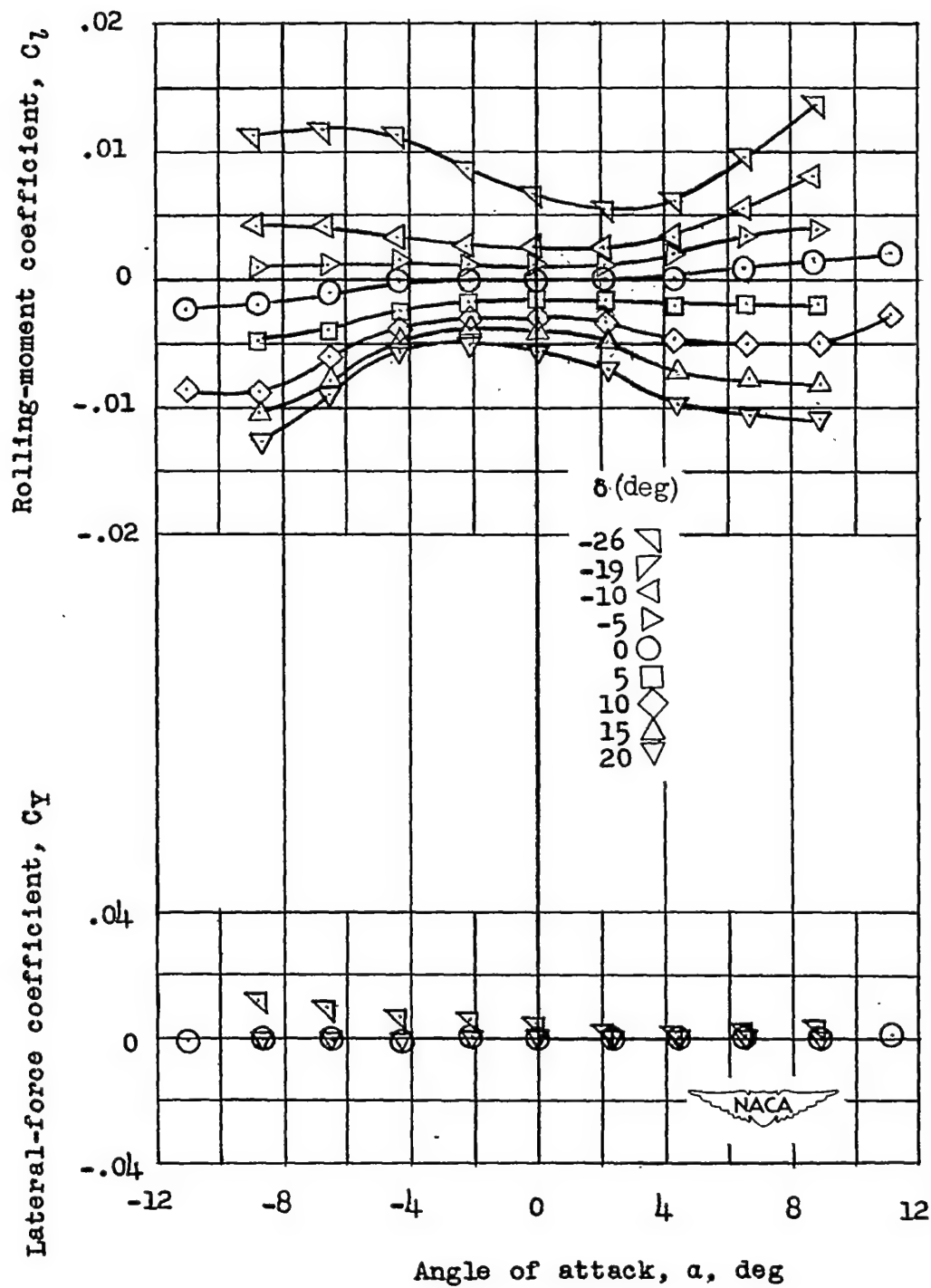
(i)   M = 0.92; R = 6.3 × 10^6.

Figure 6.- Concluded.
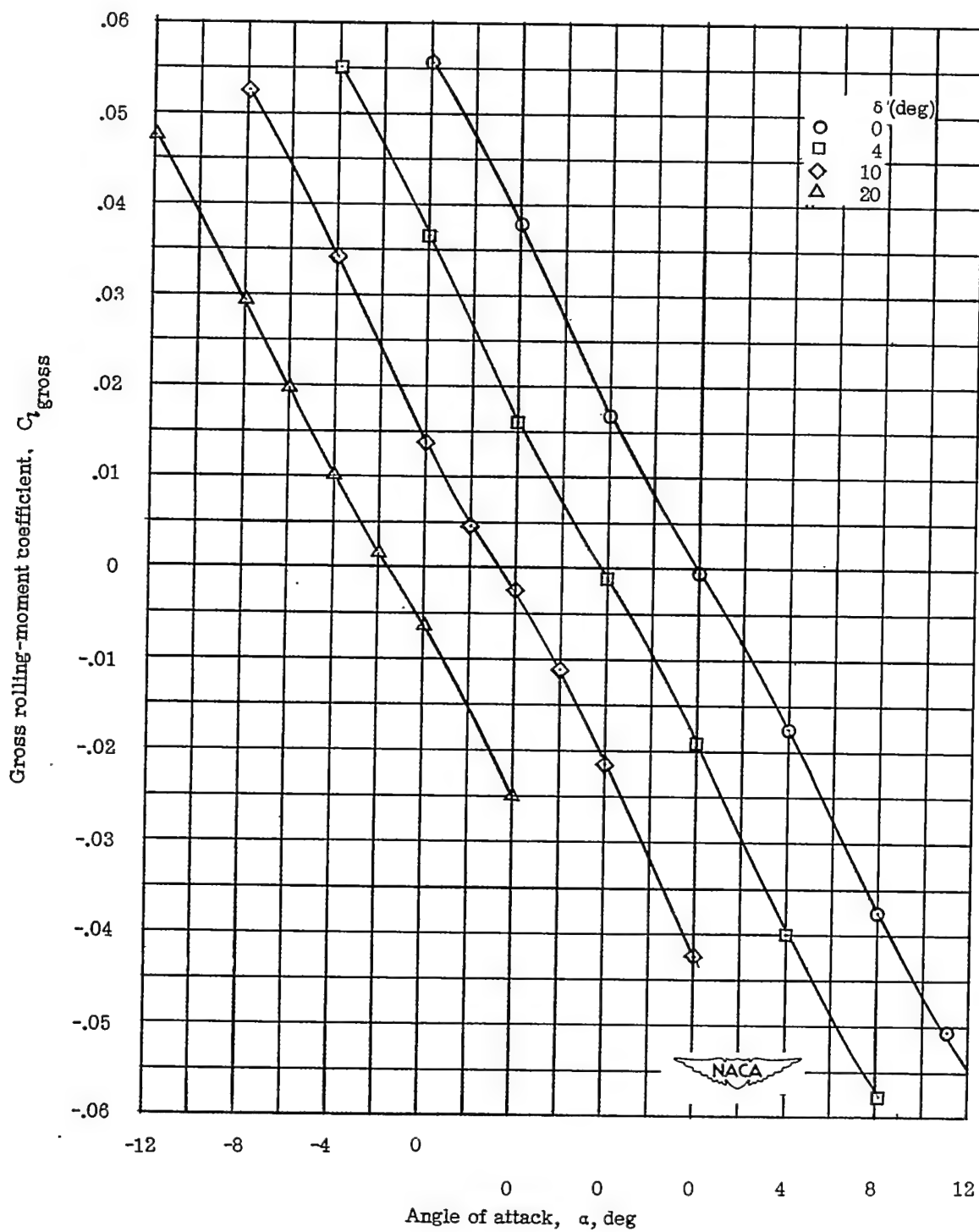
(a) M = 1.41.

Figure 7.- Gross rolling-moment characteristics of semispan model at
supersonic speeds.
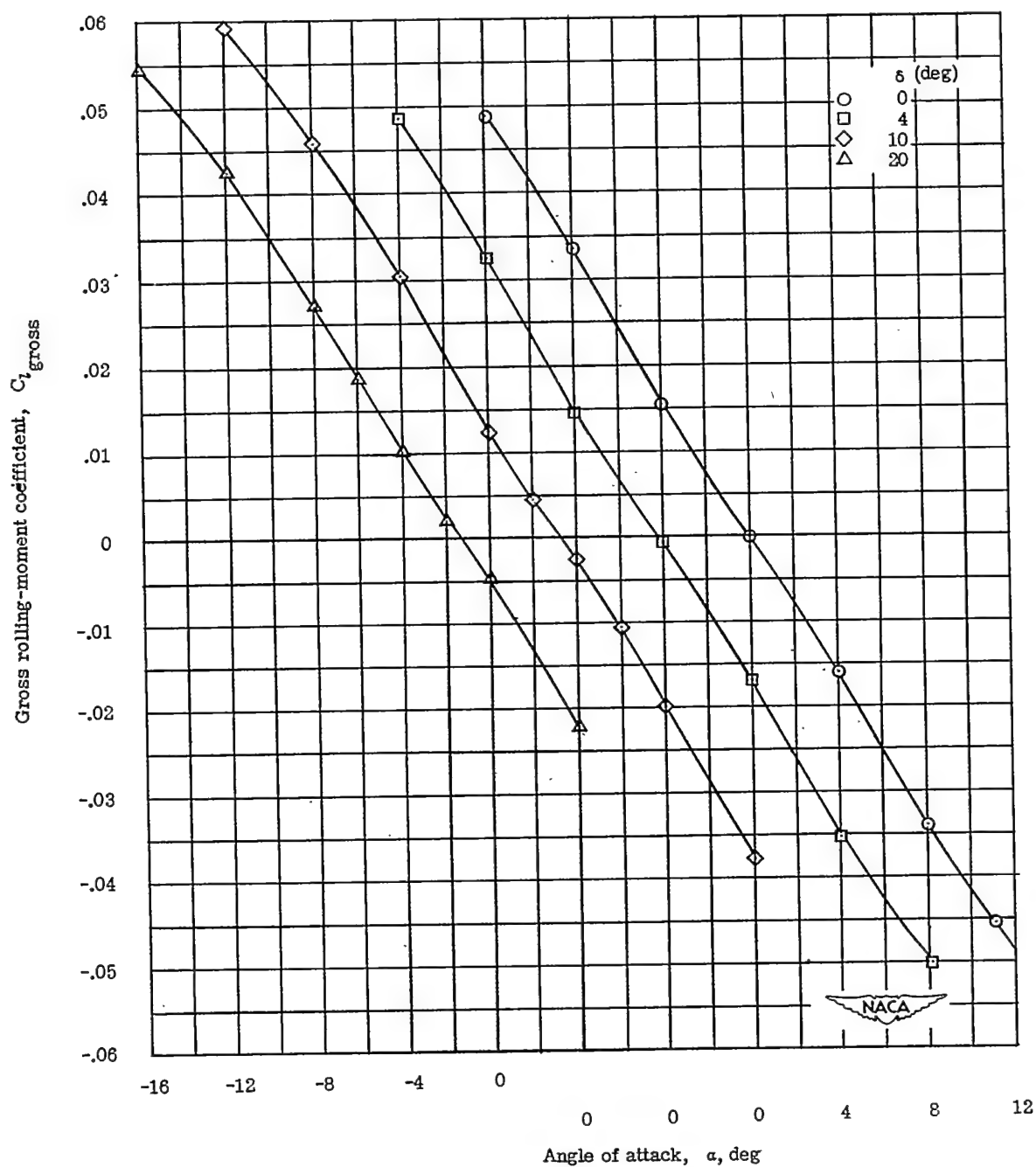
(b)   M = 1.62.

Figure 7.- Continued.
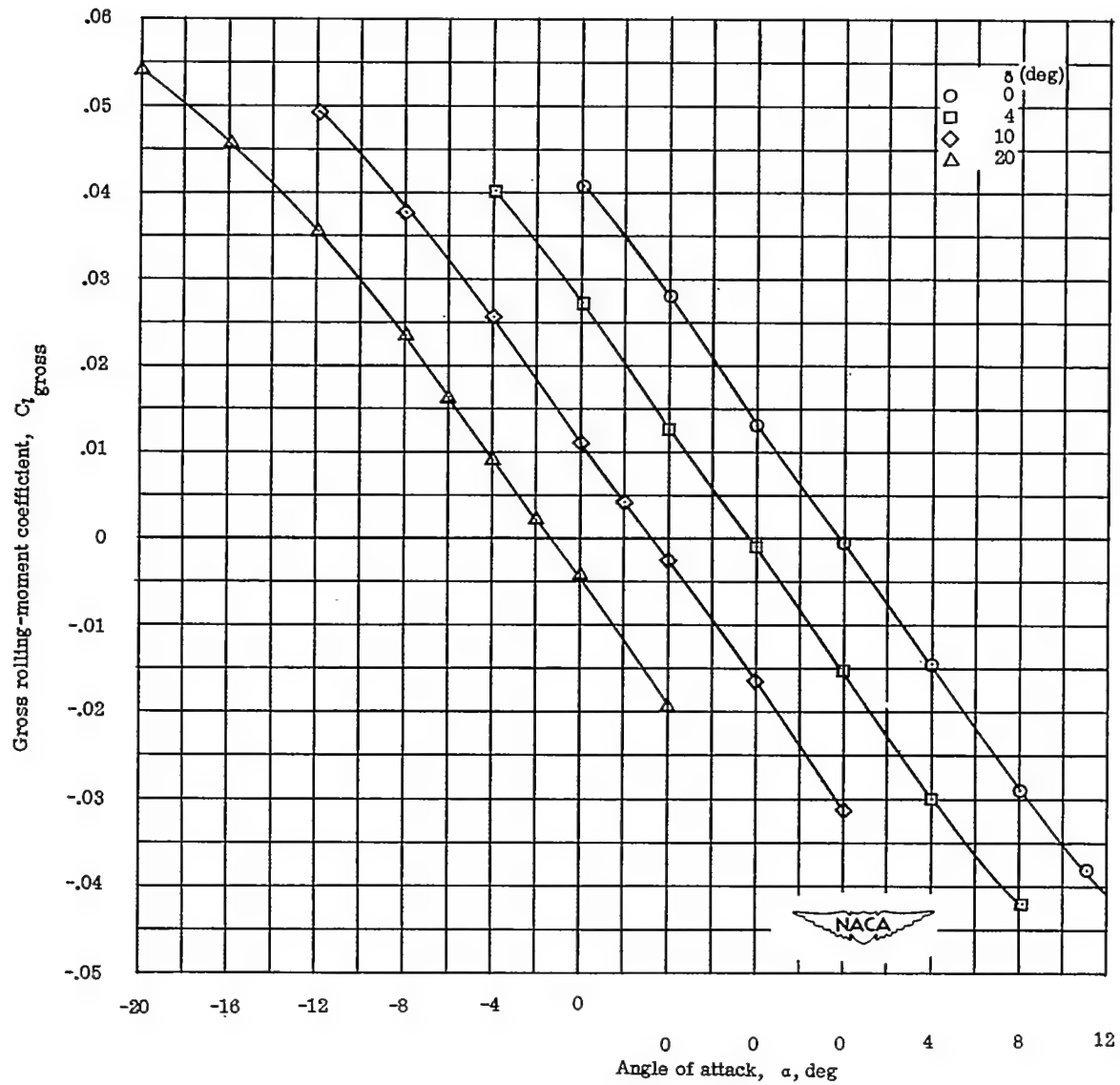
(c)   M = 1.96.

Figure 7.- Concluded.
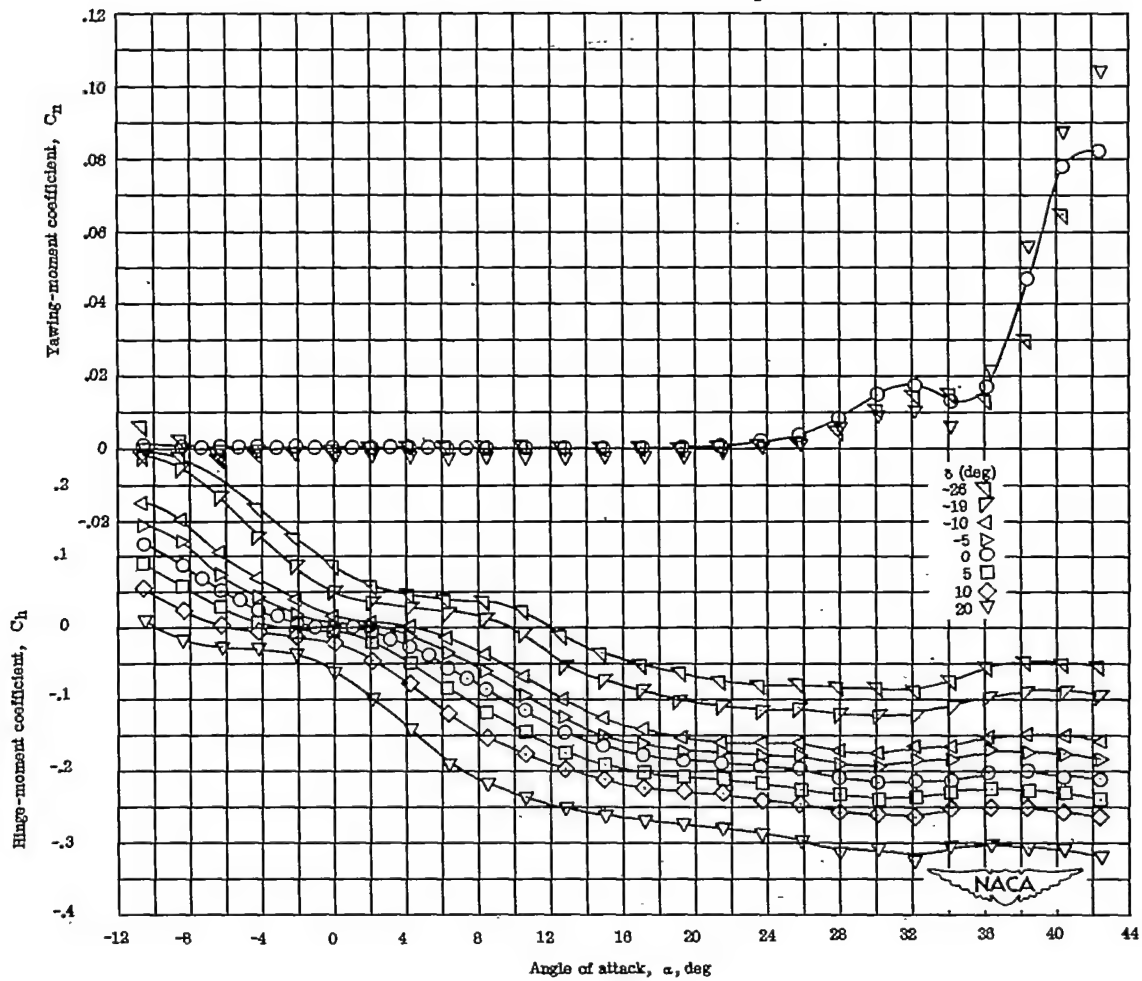
(a) M = 0.15; R = 9 × 10^6.

Figure 8.- Hinge-moment and yawing-moment characteristics at subsonic speeds.
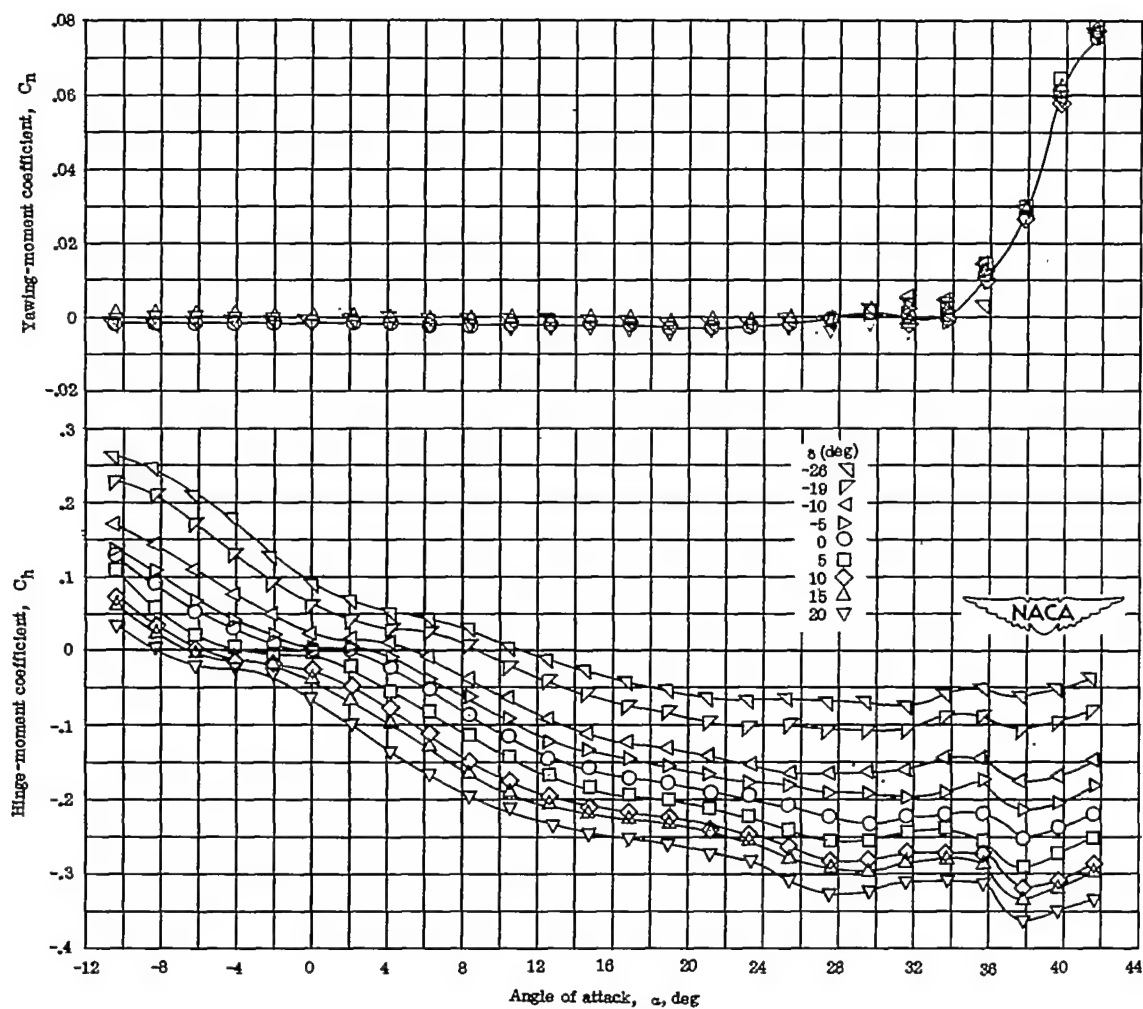
(b)　M = 0.4; R = 3.8 × 10^6.

Figure 8.- Continued.
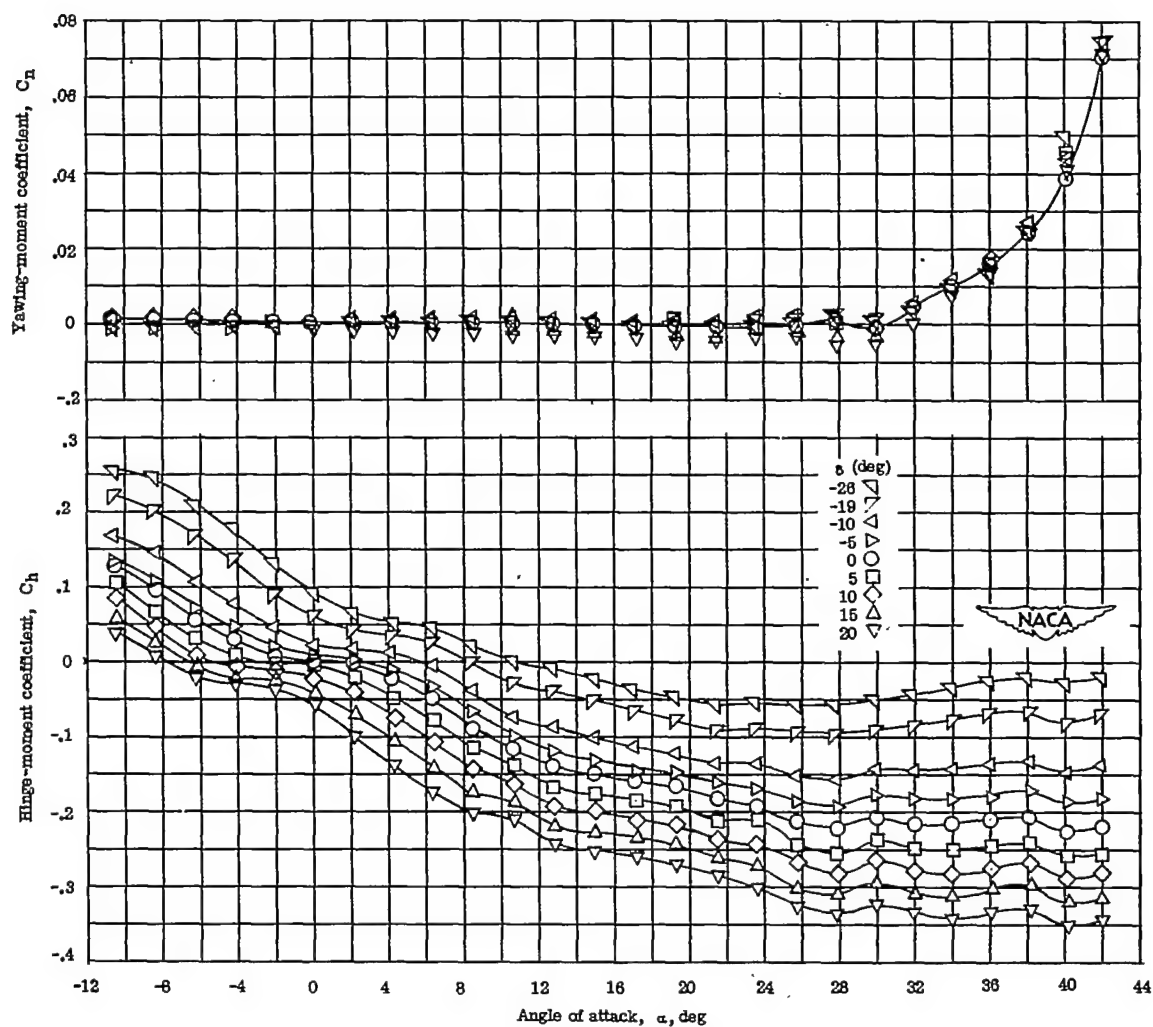
(c) M = 0.6; R = 5.1 × 10⁶.

Figure 8.- Continued.
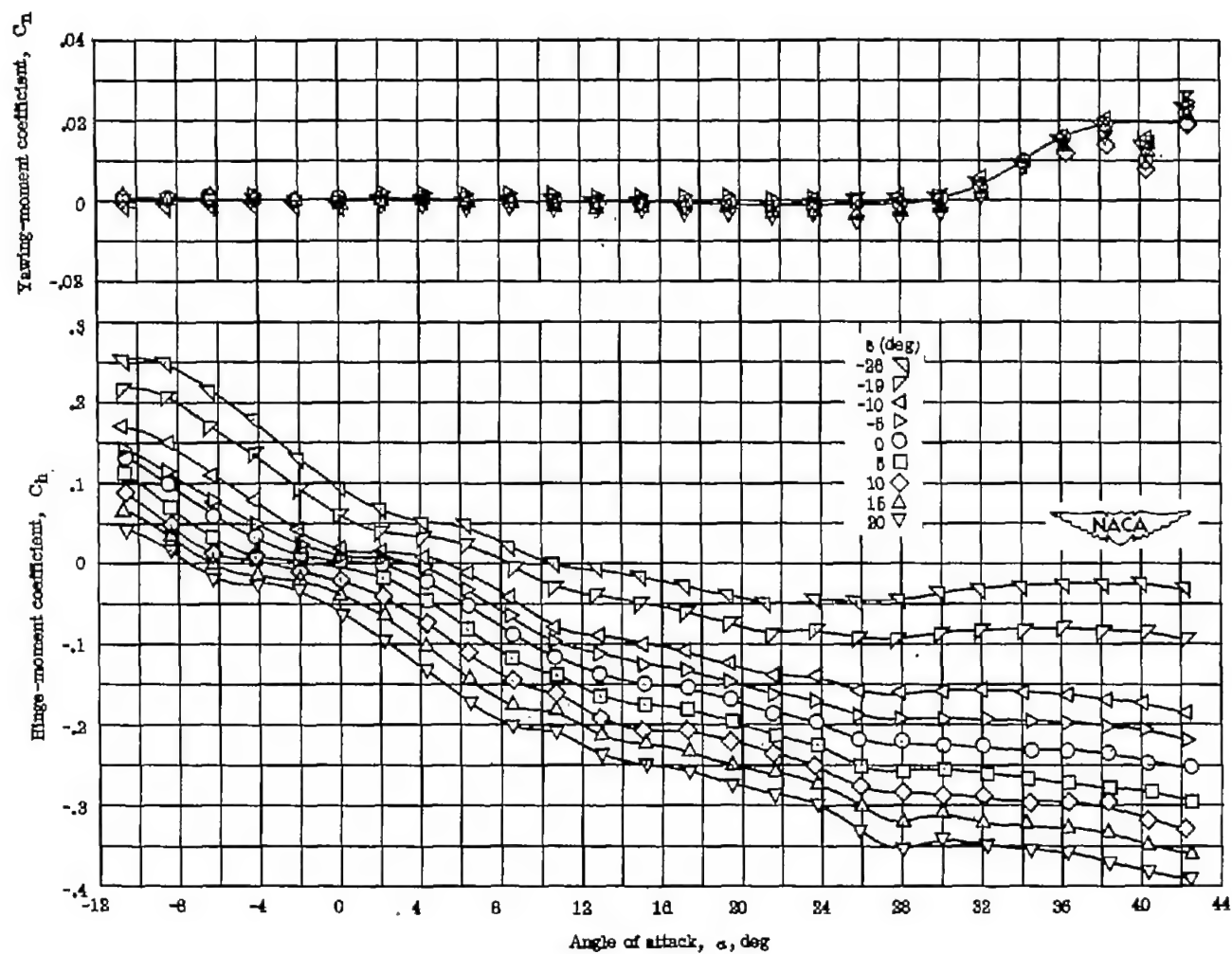
(d) M = 0.7; R = 5.5 × 10^6.

Figure 8.- Continued.
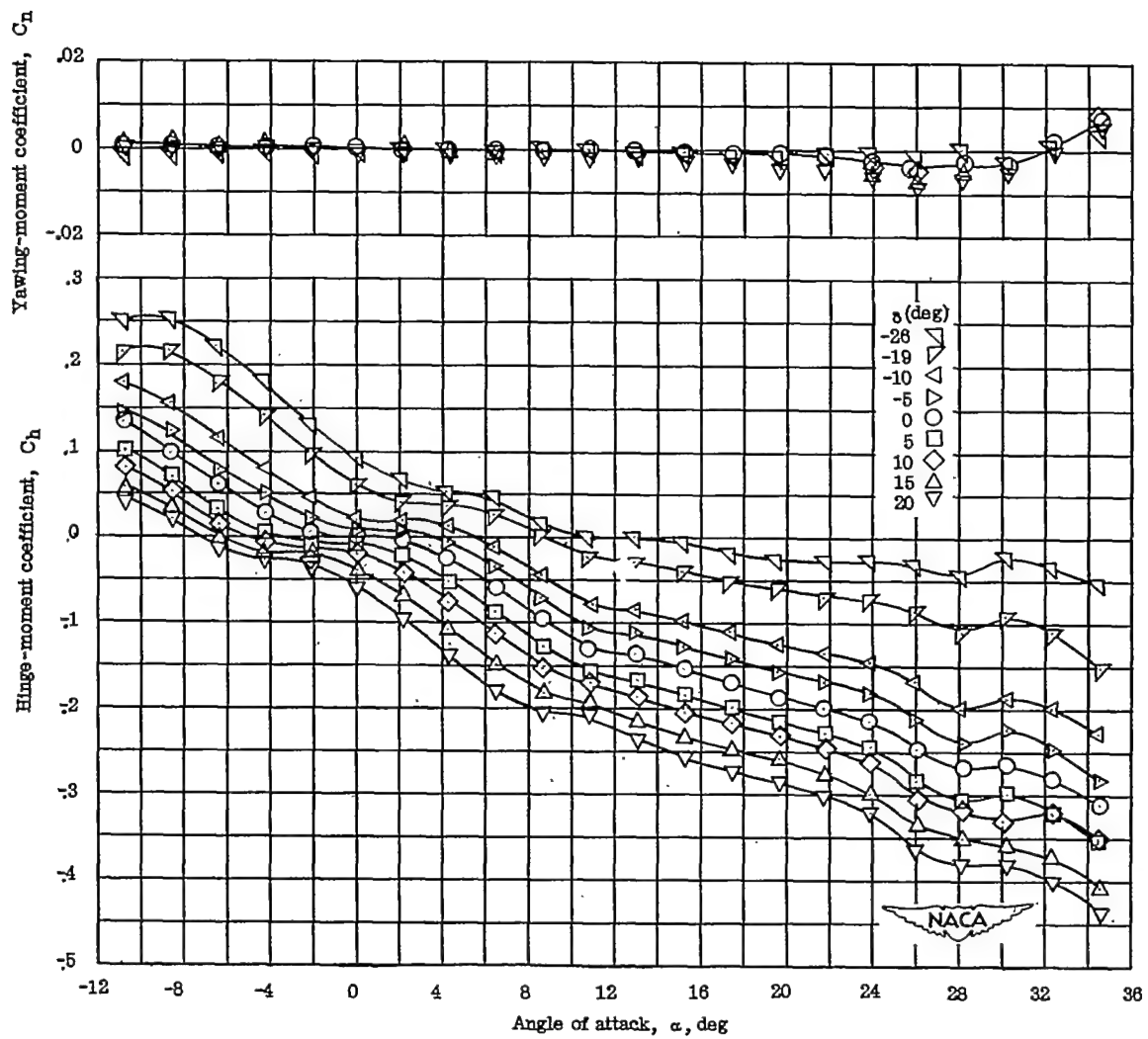
(e)   M = 0.8; R = 6 × 10⁶.

Figure 8.- Continued.
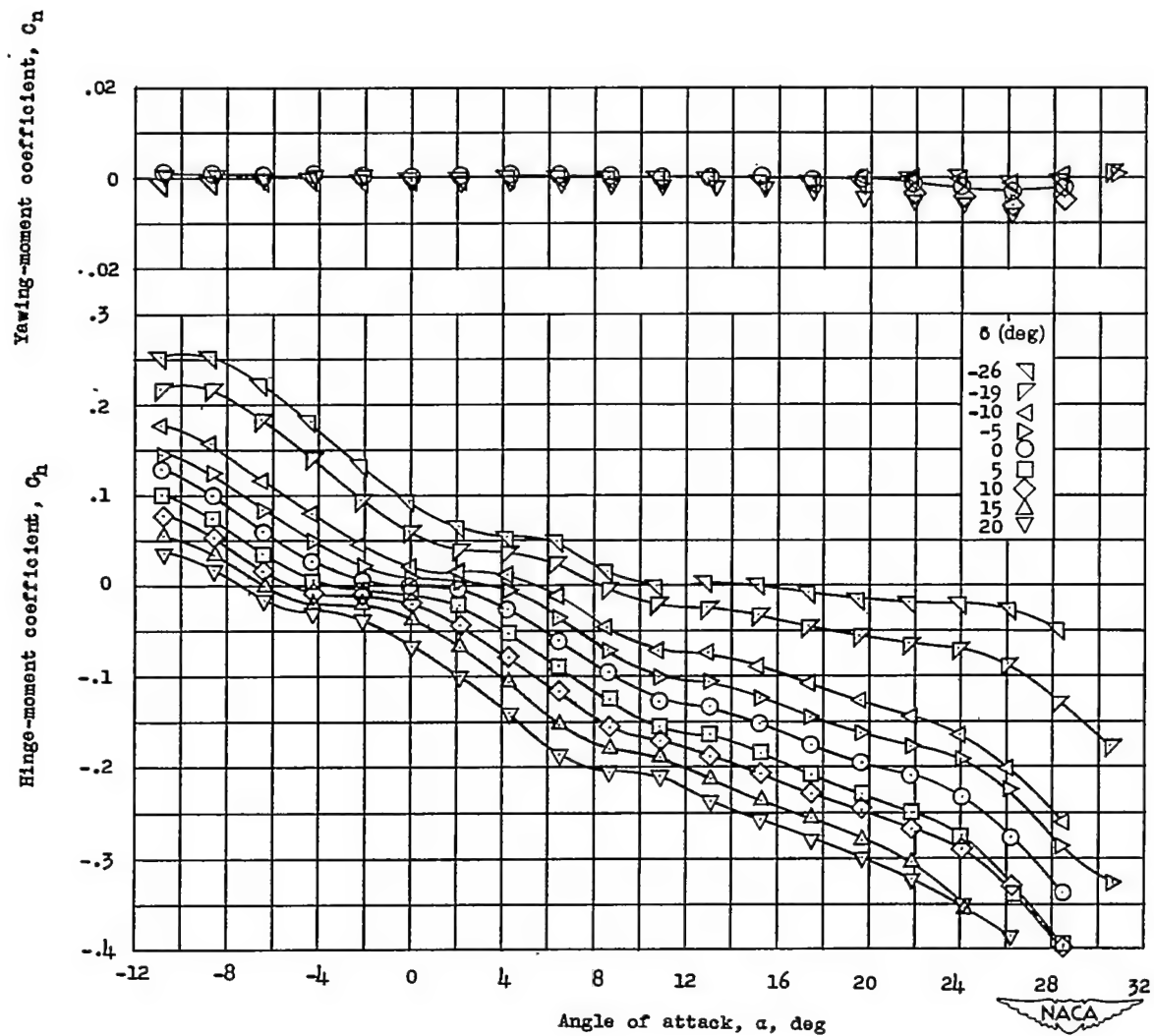
(f) M = 0.85; R = 6.1 × 10^6.

Figure 8.- Continued.
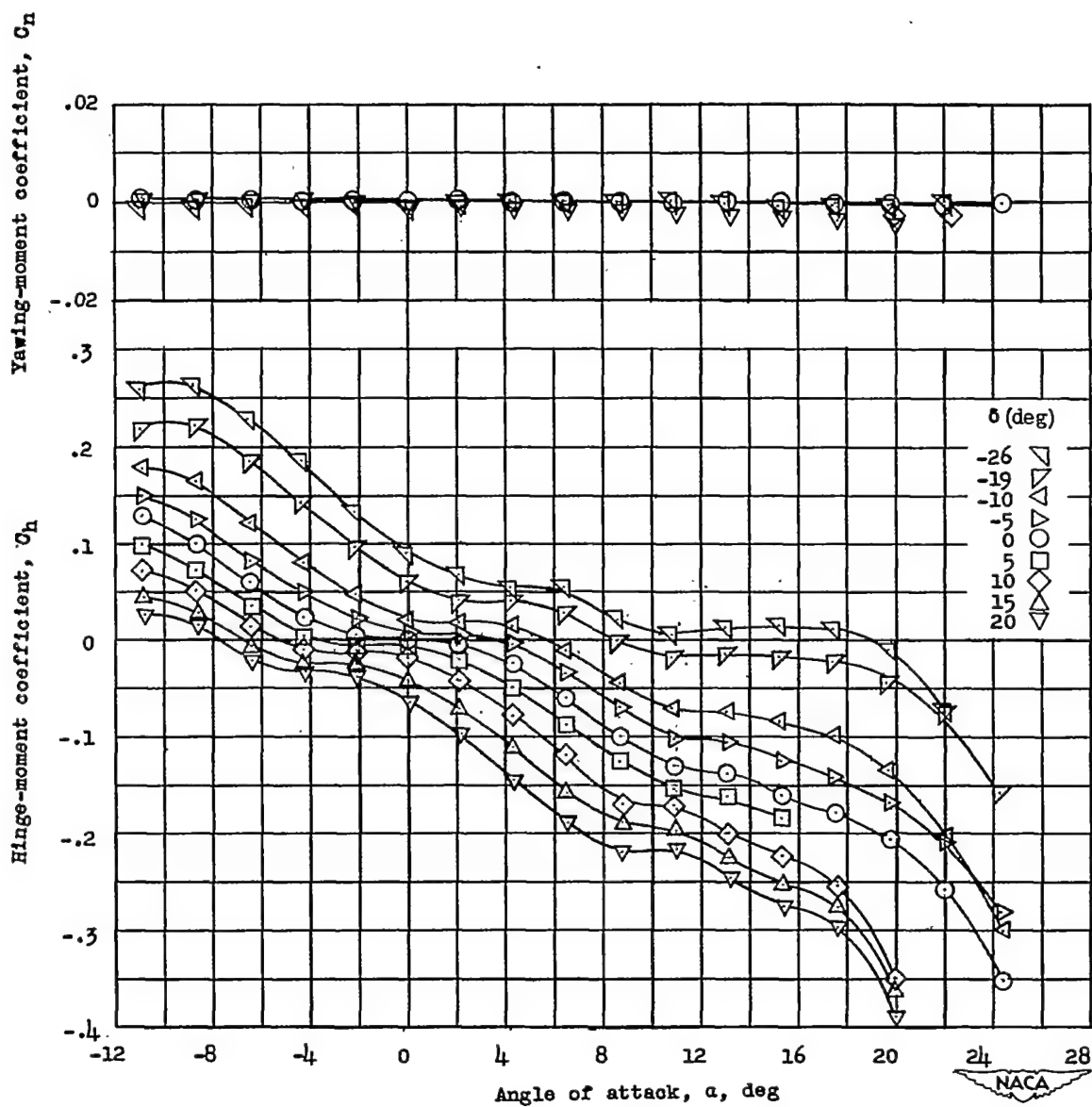
(g) $M = 0.875$; $R = 6.2 \times 10^6$.

Figure 8.- Continued.
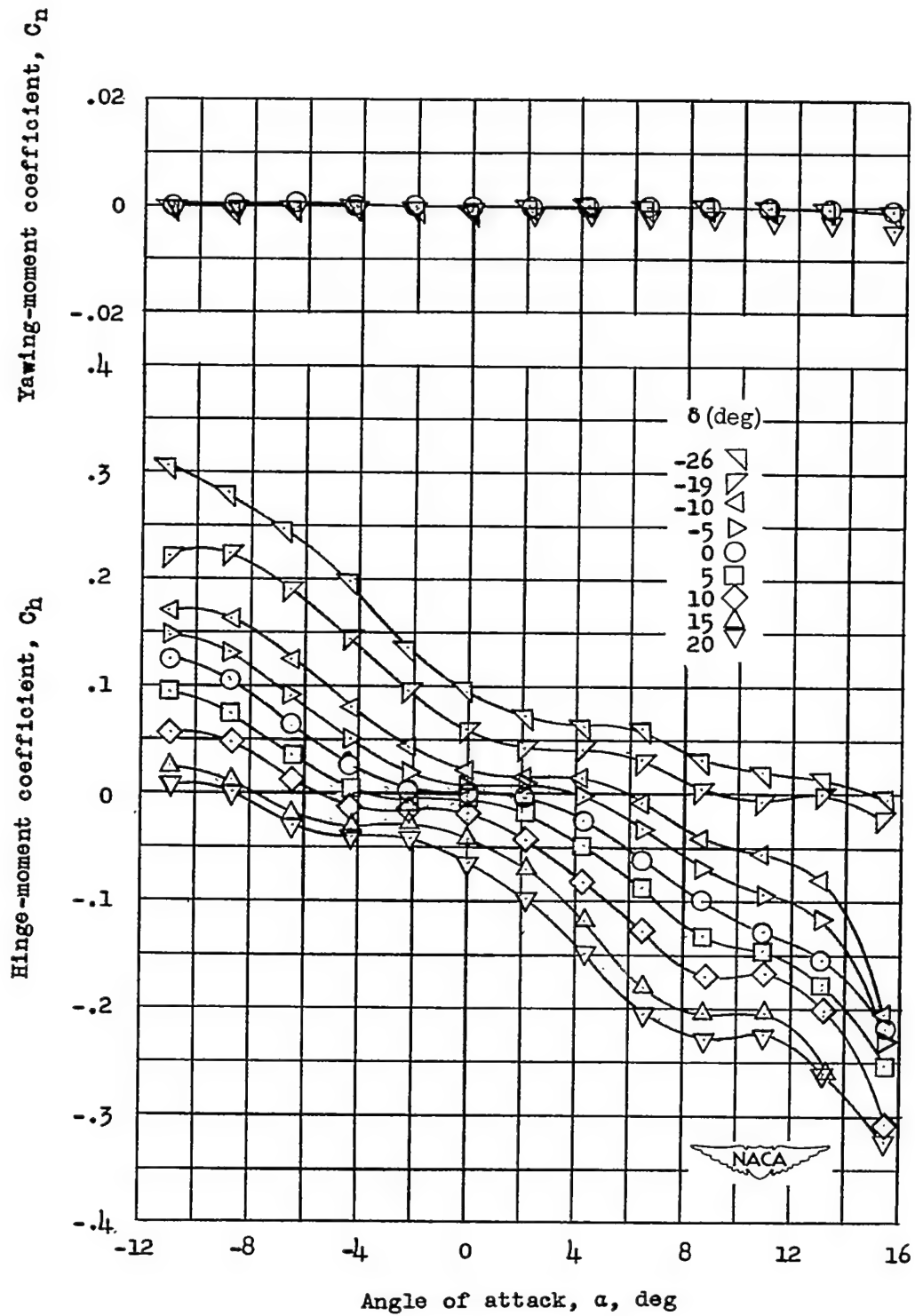
(h)   M = 0.9; R = 6.3 × 10^6.

Figure 8.- Continued.
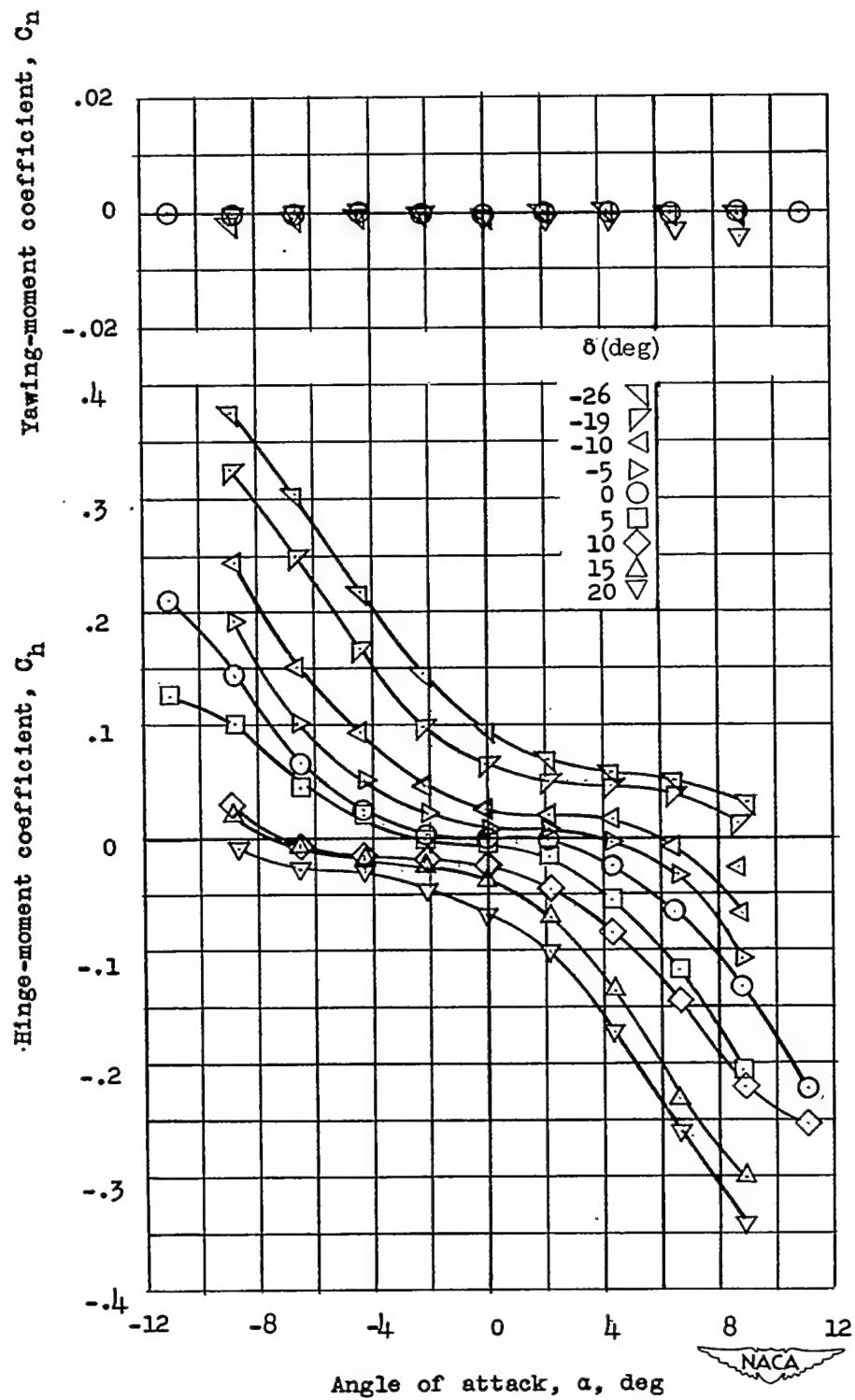
(i)　M = 0.92; R = 6.3 × 10^6.

Figure 8.- Concluded.
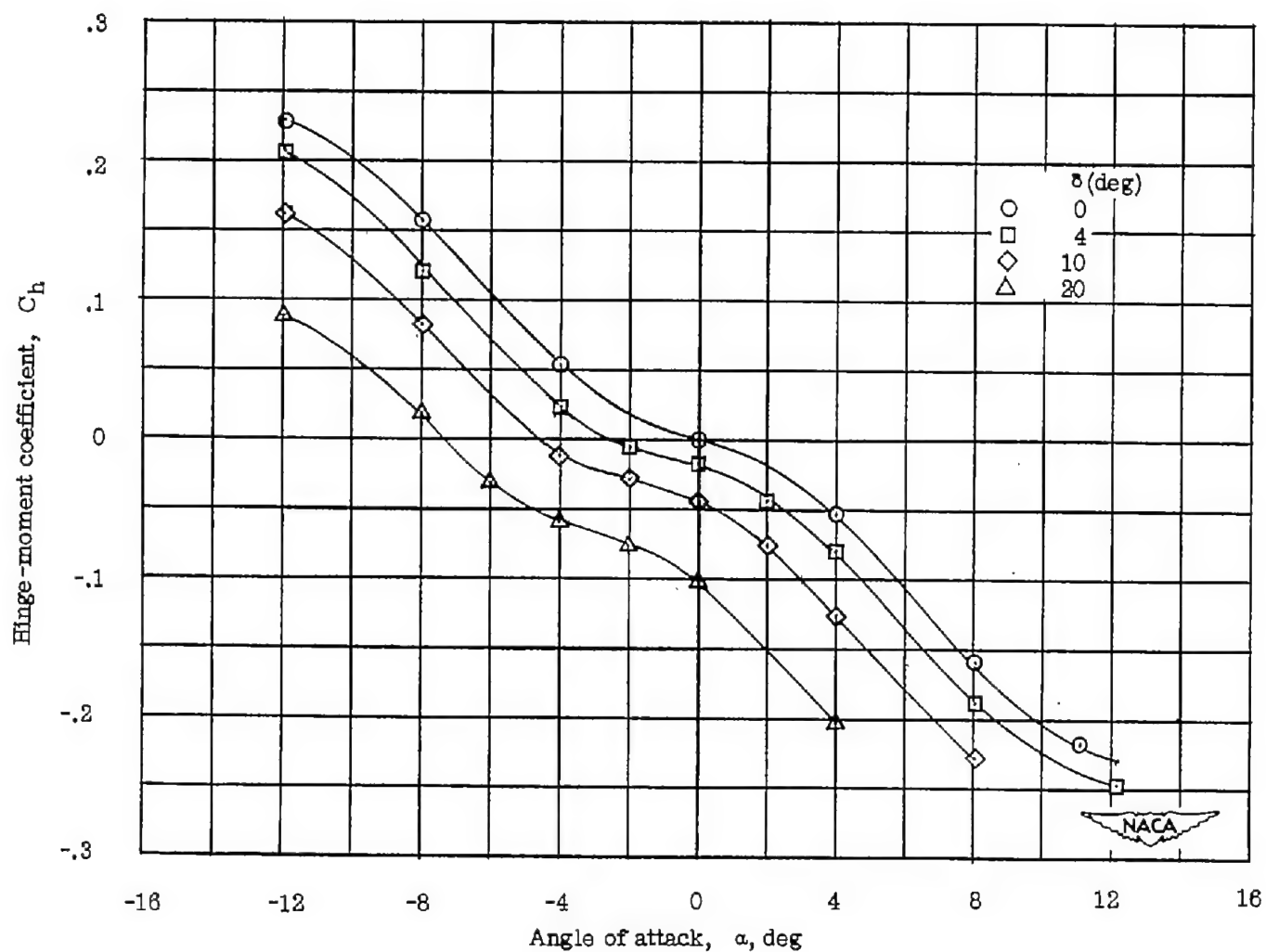
(a) M = 1.41.

Figure 9.- Control hinge moments of semispan model at supersonic speeds.
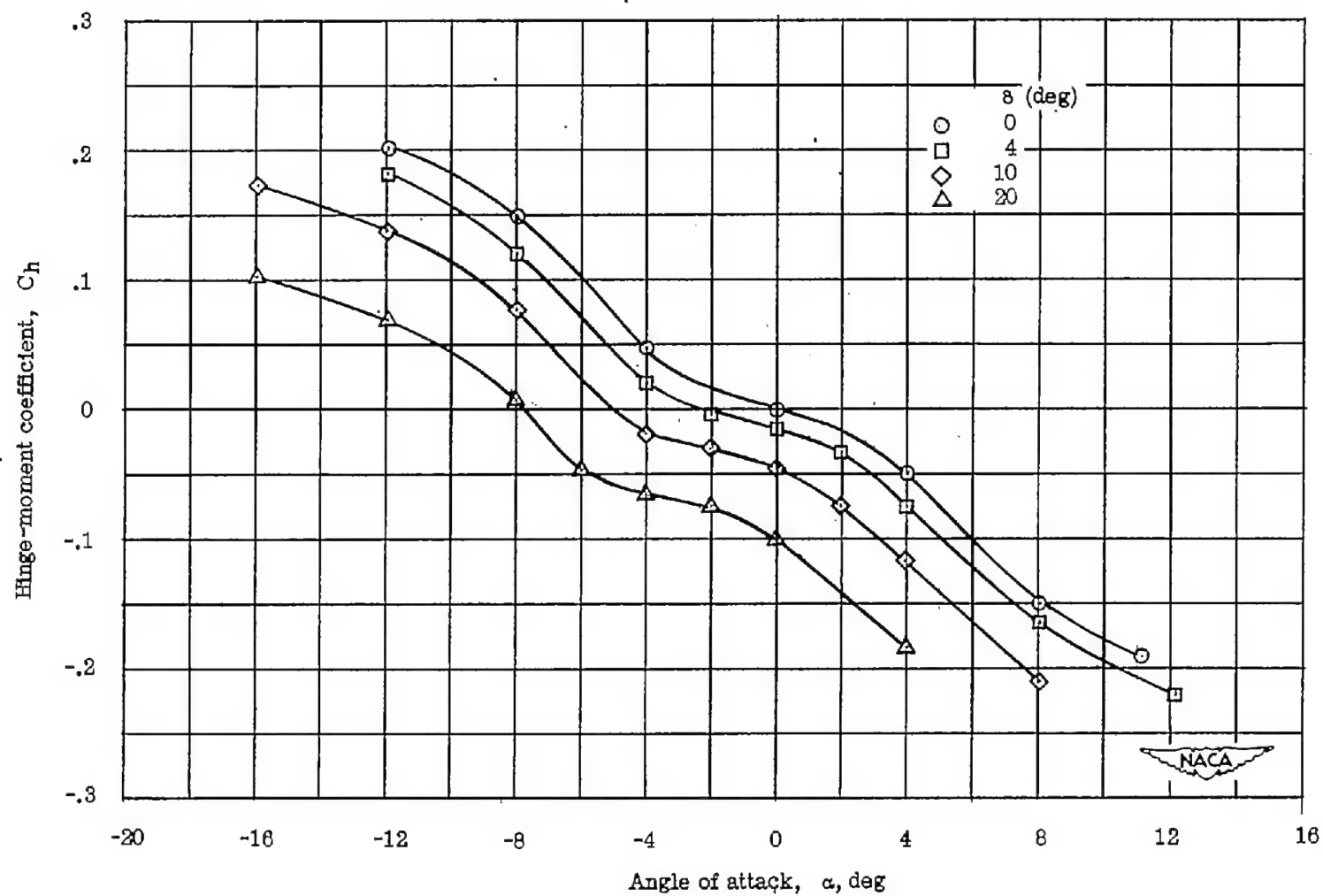
(b) M = 1.62.

Figure 9.- Continued.
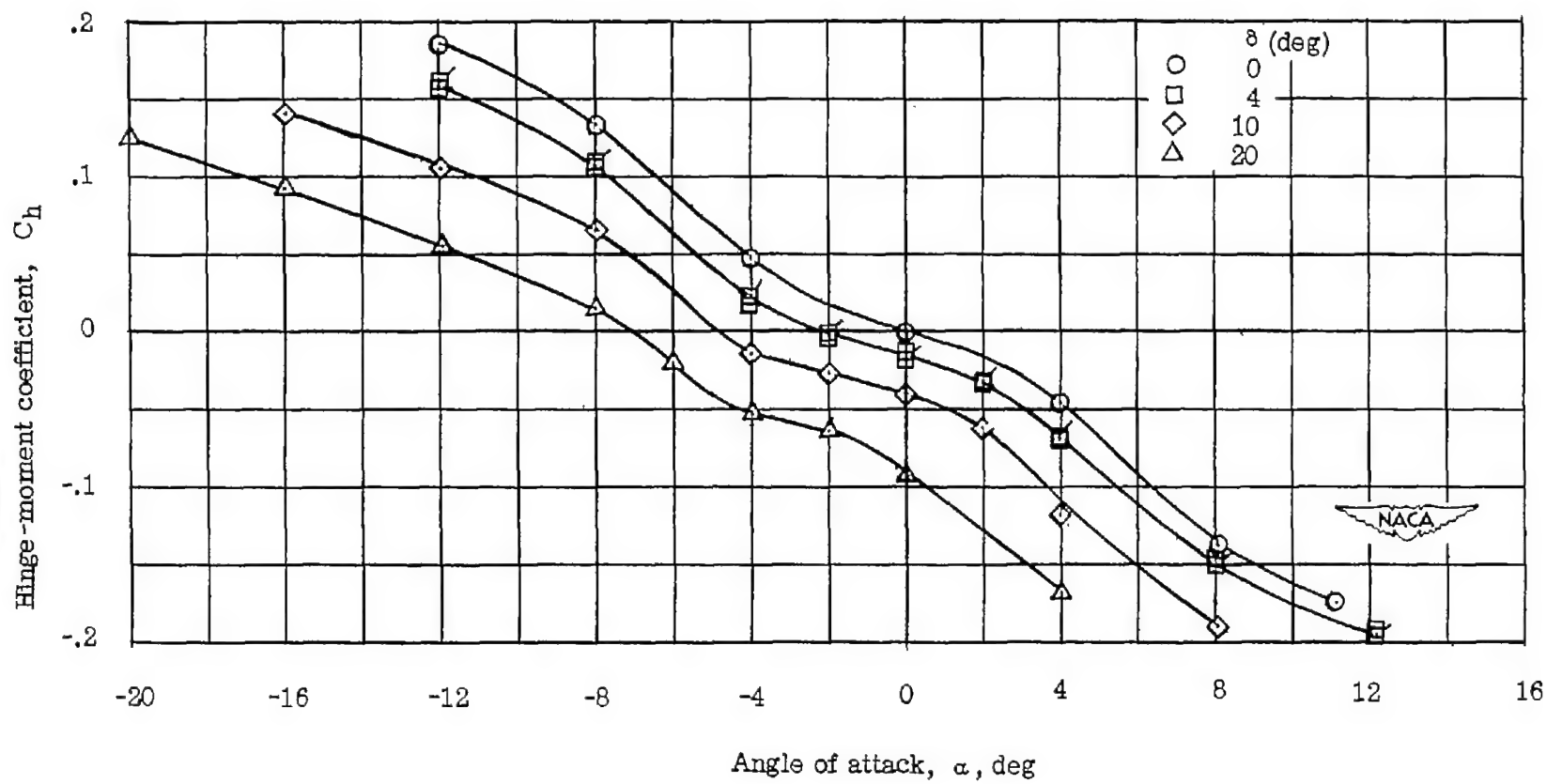
(c) M = 1.96.

Figure 9.- Concluded.
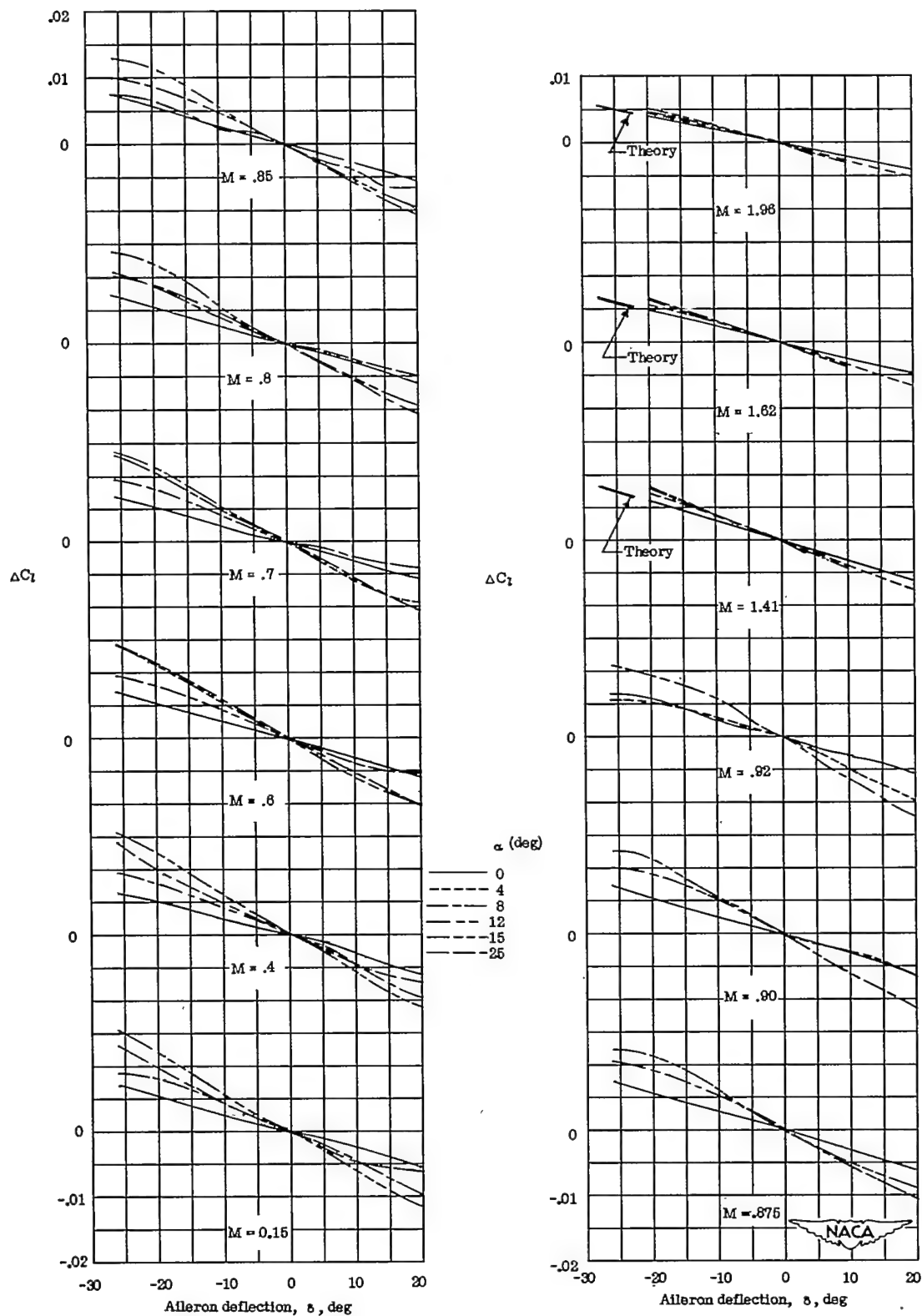
Figure 10.- Aileron rolling effectiveness at various angles of attack.
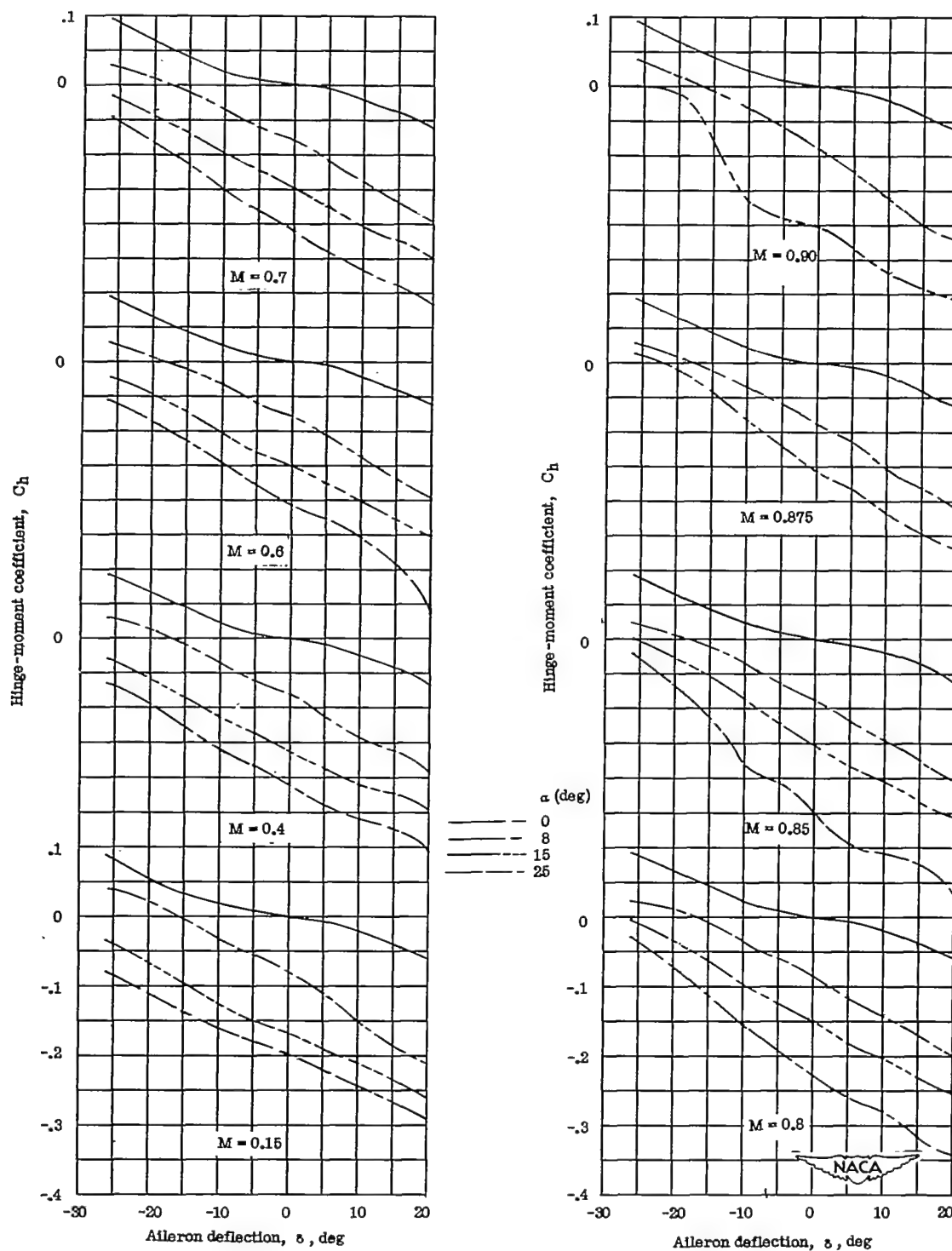
(a) Mach numbers from 0.15 to 0.90.

Figure 11.- Variation of hinge-moment coefficient with aileron deflection
at various angles of attack.
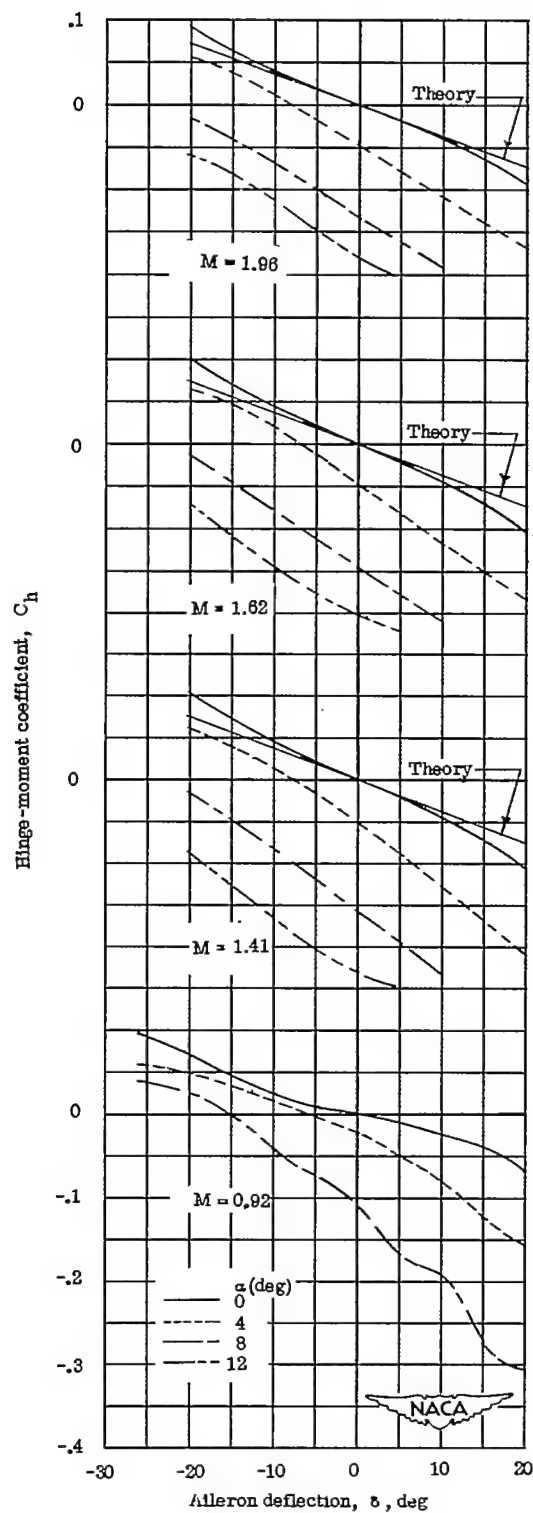
(b) Mach numbers from 0.92 to 1.96.

Figure 11.- Concluded.
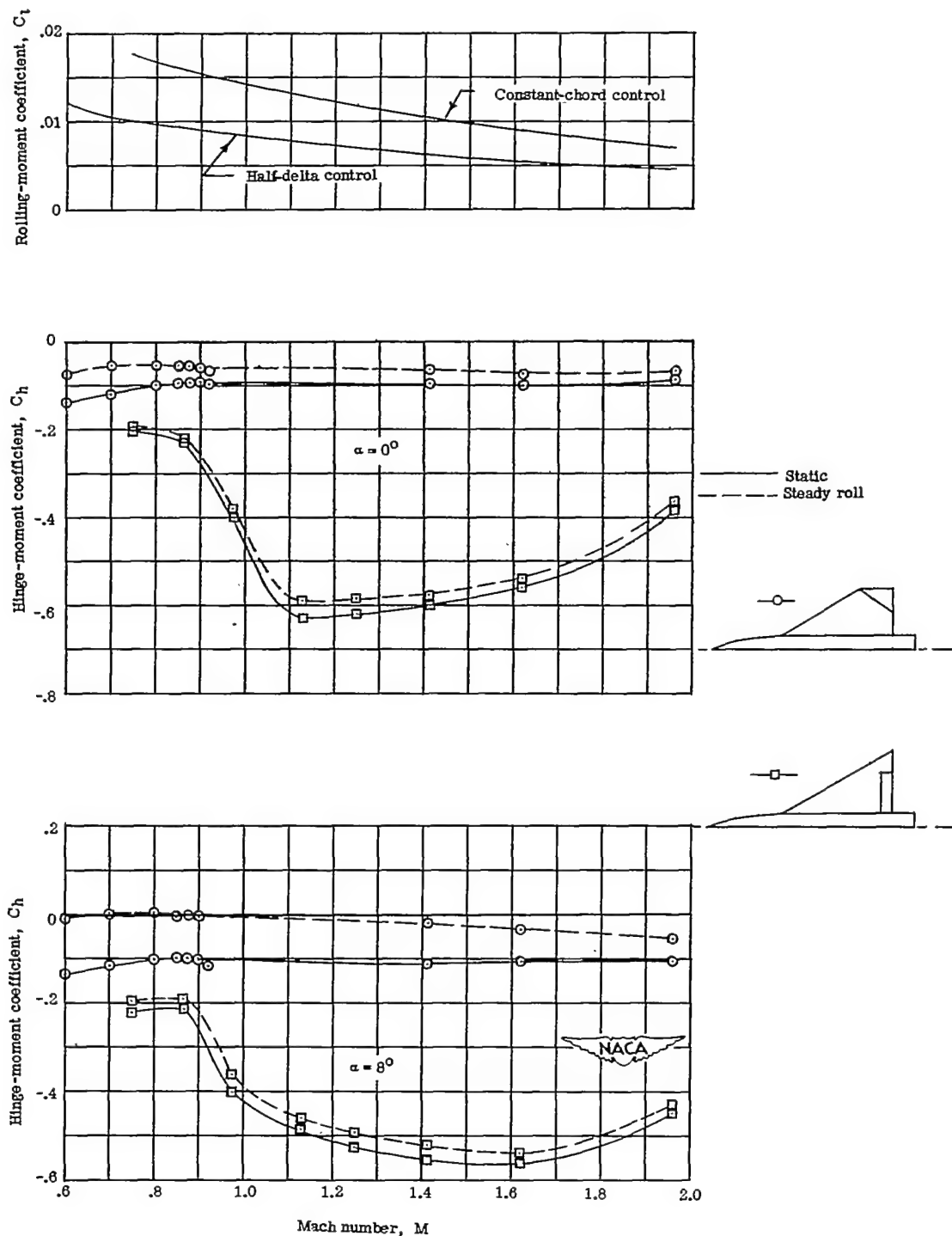
Figure 12.- Variation with Mach number of hinge-moment coefficient for subject control and comparison with similar results for an unbalanced constant-chord control on a delta wing; comparison is made at rolling moments required for 3.5 radians per second roll rates of wings having 660 square feet of area and operating at 40,000 feet.
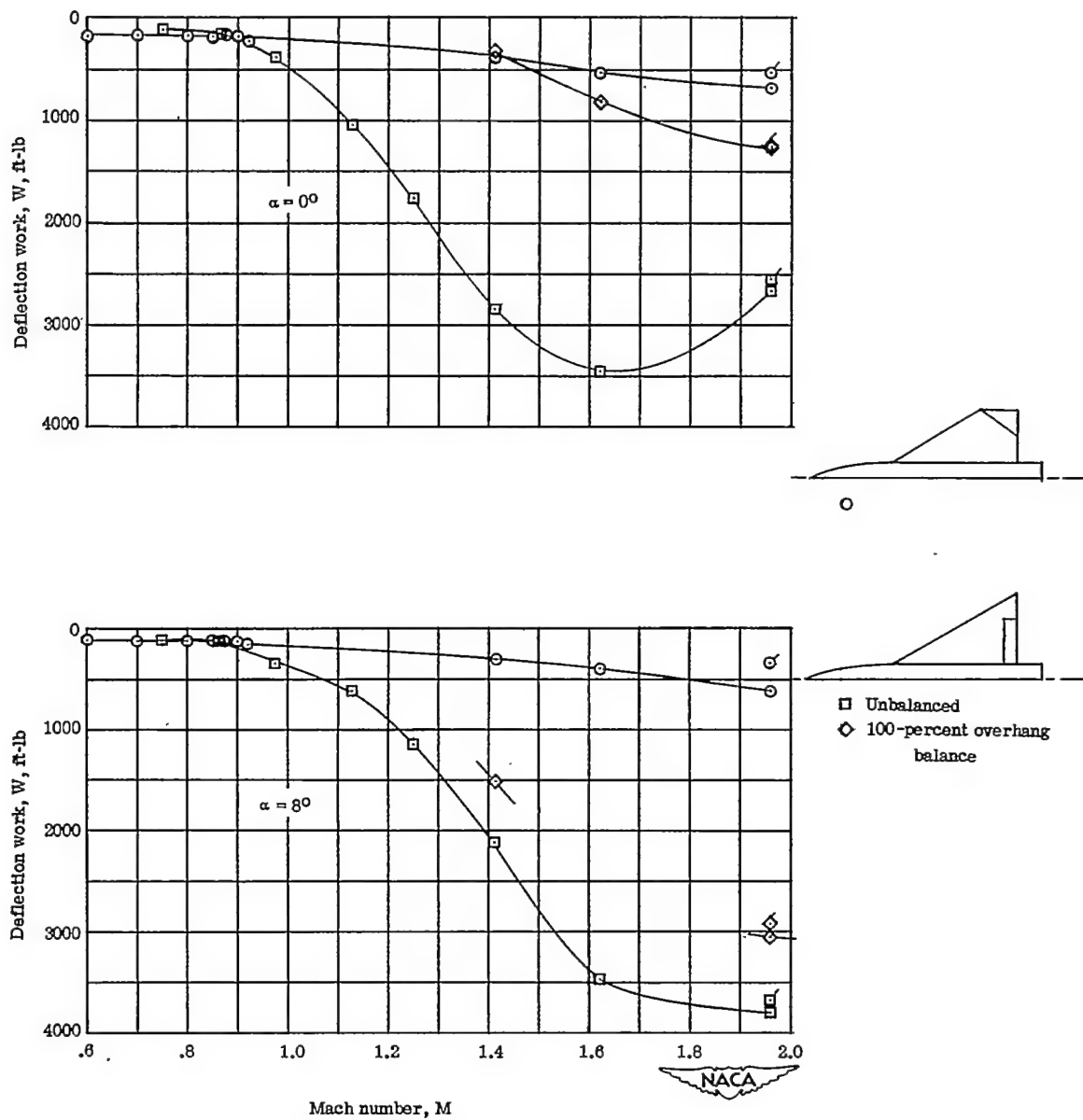
Figure 13.- Comparison of deflection work of three controls producing
rolling moments required for 3.5 radians per second roll rates of
wings having 660 square feet of area and operating at 40,000 feet.
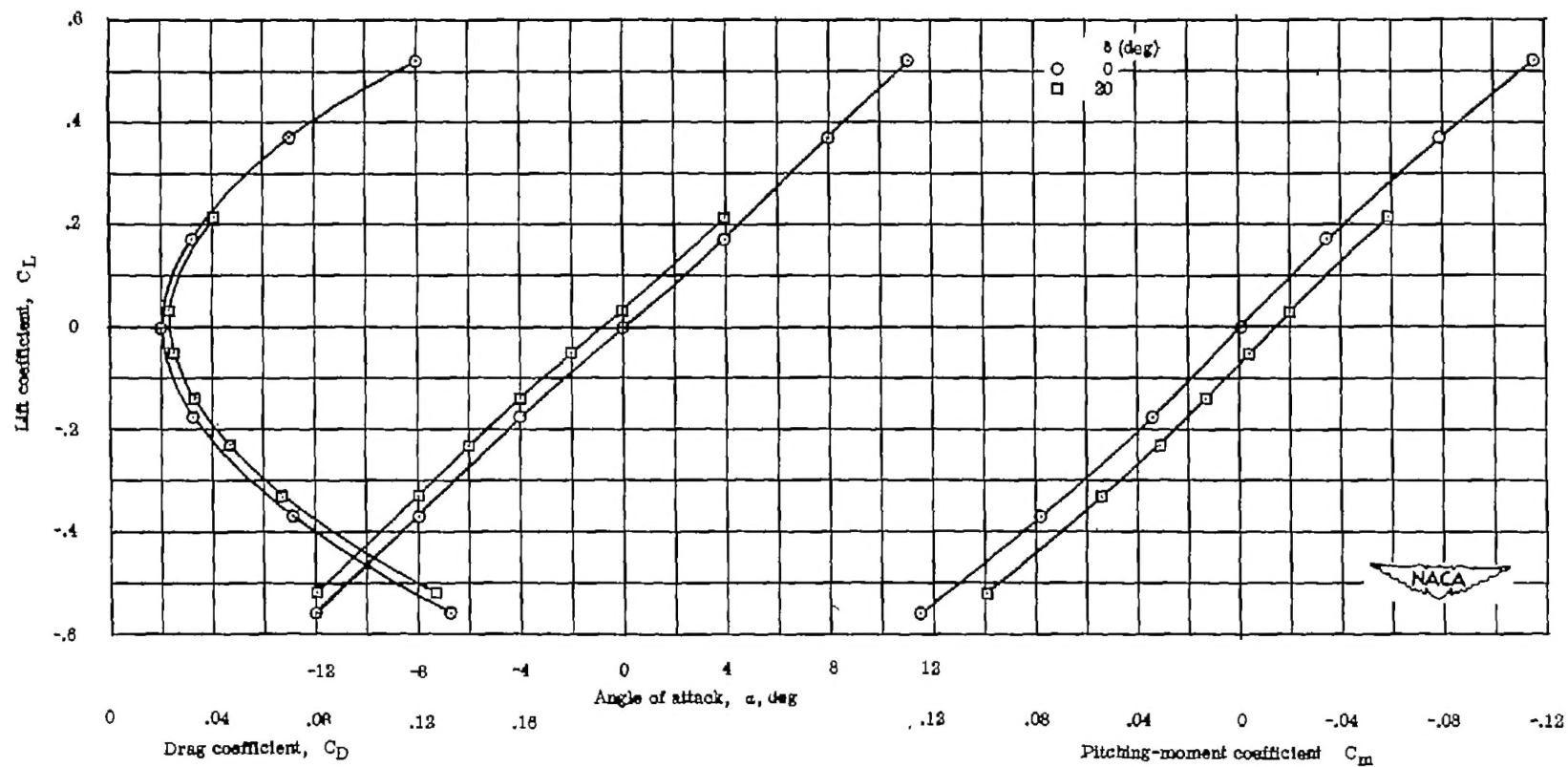Flagged symbols denote rolling case; unflagged symbols denote static
case.
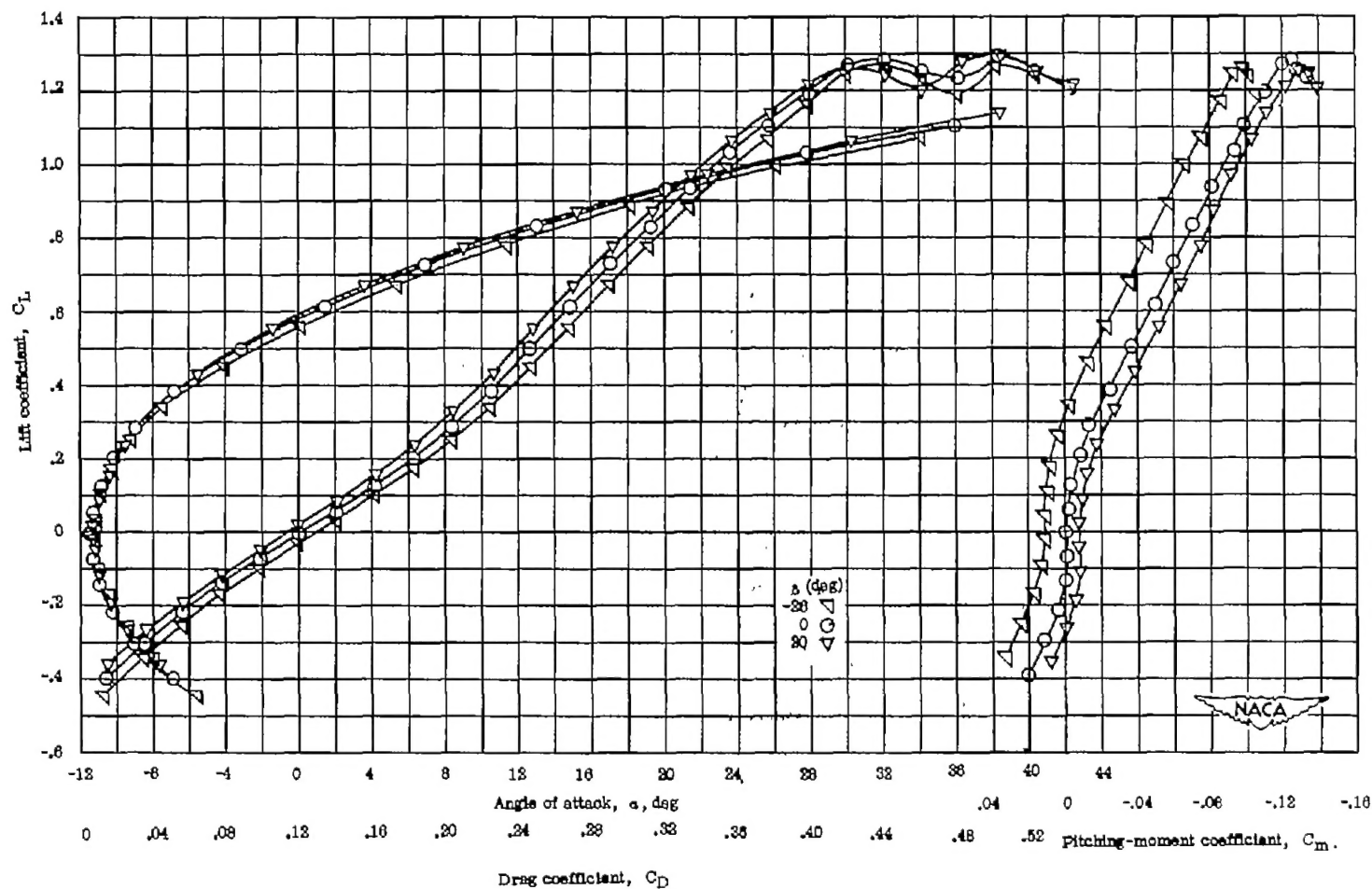
(a) M = 0.15; R = 9 × 10^6.

Figure 14.- Effect of aileron deflection on the longitudinal character-
istics at subsonic speeds.
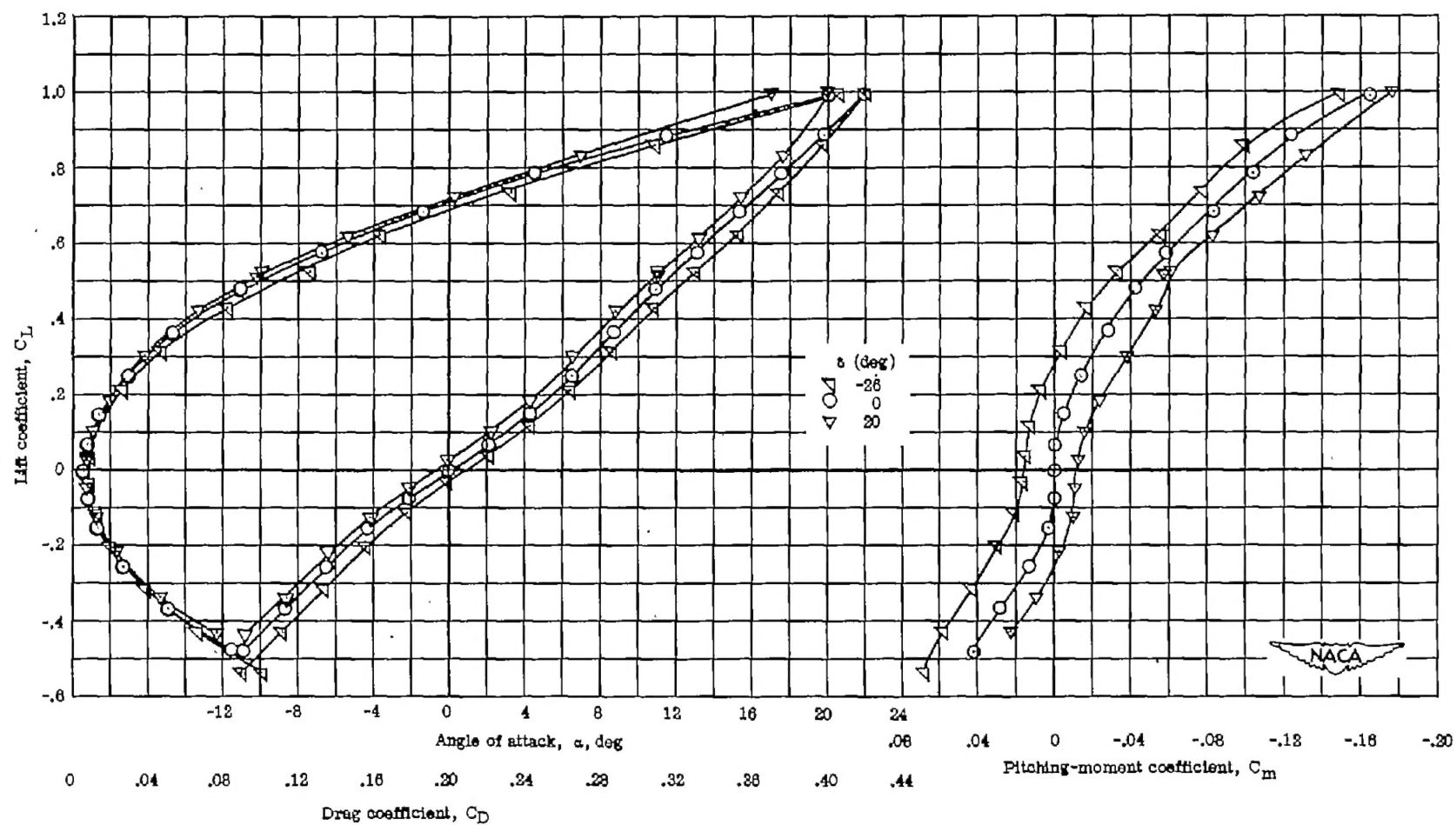
(b)   M = 0.875; R = 6.2 × 10⁶.

Figure 14.- Concluded.

(a) M = 1.41.

Figure 15.- Representative lift, drag, and pitching-moment data of
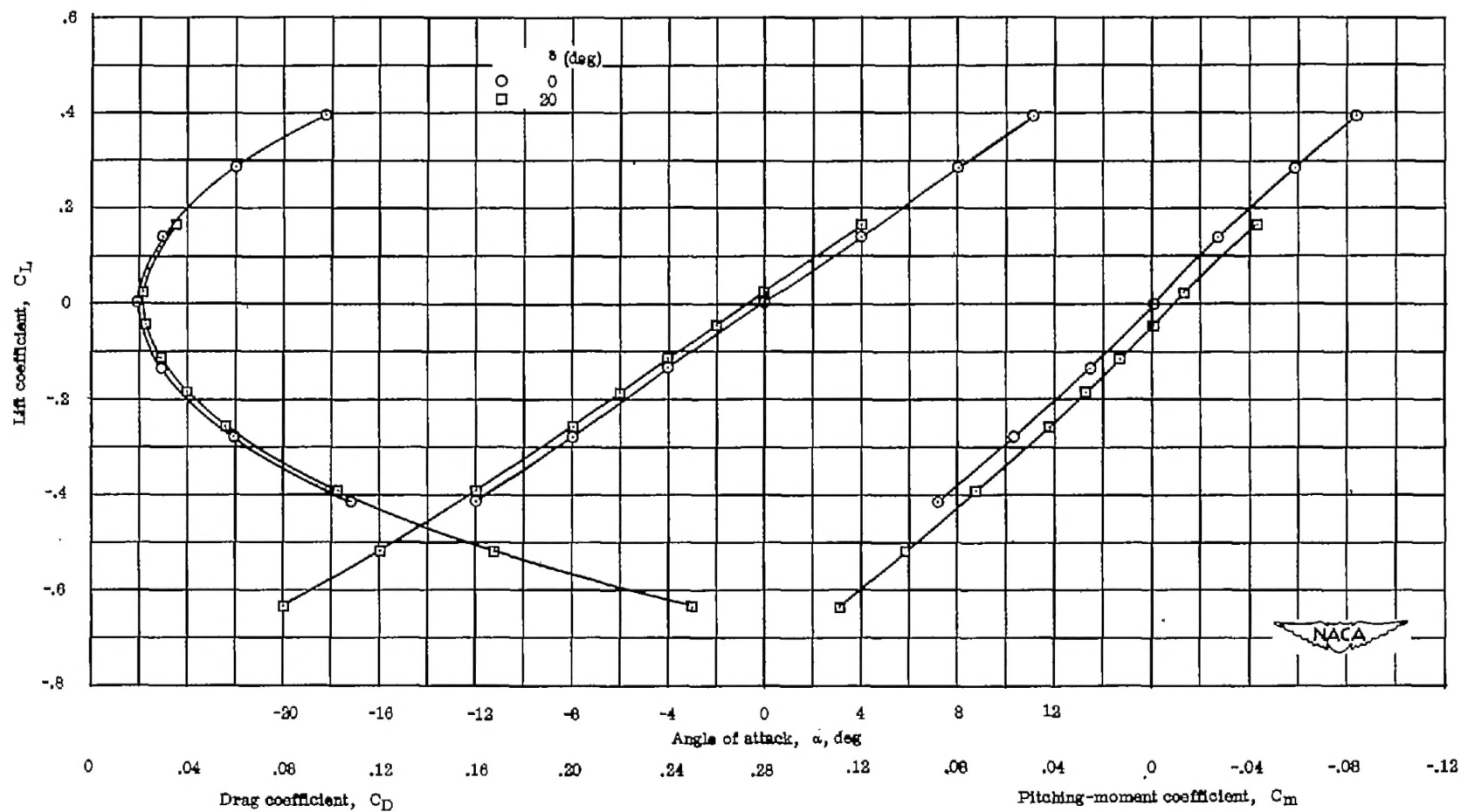semispan model at supersonic speeds.

(b) M = 1.96.

Figure 15.- Concluded.